THE EFFECT OF IMPLANT CONFORMITY ON MUSCLE FORCE REQUIREMENTS IN THE IMPLANTED KNEE

by

Grace McConnochie

A thesis

submitted in partial fulfillment

of the requirements for the degree of

Master of Science in Mechanical Engineering

Boise State University

August 2019

BOISE STATE UNIVERSITY GRADUATE COLLEGE

DEFENSE COMMITTEE AND FINAL READING APPROVALS

of the thesis submitted by

Grace McConnochie

Thesis Title: The Effect of Implant Conformity on Muscle Force Requirements in the Implanted Knee

Date of Final Oral Examination: 15 March 2019

The following individuals read and discussed the thesis submitted by student Grace McConnochie, and they evaluated her presentation and response to questions during the final oral examination. They found that the student passed the final oral examination.

Clare K. Fitzpatrick, Ph.D.	Chair, Supervisory Committee
Tyler N. Brown, Ph.D.	Member, Supervisory Committee
Gunes Uzer, Ph.D.	Member, Supervisory Committee

The final reading approval of the thesis was granted by Clare K. Fitzpatrick, Ph.D., Chair of the Supervisory Committee. The thesis was approved by the Graduate College.

DEDICATION

Dedicated to my family for all their support.

ACKNOWLEDGEMENTS

Many thanks to Dr. Clare K. Fitzpatrick for the opportunity to pursue this research, along with support, mentorship and advice throughout my academic career. I would also like to thank Dr. Tyler Brown and Dr. Gunes Uzer for participating on my thesis committee and for providing valuable guidance and feedback. And a special thanks to my colleagues in the Computational Biosciences Lab for helpful discussions and instructions.

ABSTRACT

Implant geometry is a significant factor in determining knee stability and patient satisfaction following total knee replacement (TKR). Ineffective muscle recruitment, impaired joint functionality and increased implant wear are consequences of an unstable knee replacement. Current knee laxity evaluation techniques are limited in their ability to account for the muscular response to knee instability. This study utilizes a subject-specific lower-body musculoskeletal finite element (FE) model with dynamic muscle loading to evaluate implant laxity during activities of daily living. The effect of varying implant conformity on the muscle forces required to maintain a target kinematic profile during simulated laxity testing were quantified here for the first time. With increasing implant conformity, muscle force requirements to maintain target kinematics were significantly reduced – on average, as implant conformity increased by 0.1, muscle force requirements were reduced by 10.4%. As expected, contact mechanics of the tibiofemoral joint was also altered with implant conformity – increased conformity resulted in higher contact area and lower contact pressure. The strength of correlation between muscle force and implant conformity was shown to be activity-dependent, with more demanding activities showing a stronger correlation between muscle force and implant conformity. This is a unique and, we believe, insightful approach to assessing the effect of implant geometry on musculoskeletal demands and may have significant and sustained impact on prescribed treatment options for knee osteoarthritis.

TABLE OF CONTENTS

LIST OF TABLES

LIST OF FIGURES

LIST OF ABBREVIATIONS

1D	One-Dimensional
2D	Two-Dimensional
3D	Three-Dimensional
AP	Anterior-Posterior
ALC	Anterior Lateral Capsule
alPCL	Anterior-Lateral Bundles of the PCL
CR	Conformity Ratio
DOF	Degrees of Freedom
FE	Finite Element
IE	Internal-External
LCL	Lateral Collateral Ligament
LPFL	Lateral Patellofemoral Ligament
ML	Medial-Lateral
MPFL	Medial Patellofemoral Ligament
MS	Musculoskeletal
OA	Osteoarthritis
PCAPL	Lateral Posterior Capsule
PCAPM	Medial Posterior Capsule
PF	Patellofemoral
PFL	Lateral Popliteofibular ligament

PI	Proportional–Integral
pmPCL	Posterior-Medial Bundles of the PCL
PT	Patella Tendon
RMS	Root Mean Square
sMCL	Superficial Medial Collateral Ligament
STD	Standard Deviation
TF	Tibiofemoral
TKR	Total Knee Replacement

CHAPTER ONE : INTRODUCTION

1.1 A brief overview of total knee replacement procedure and loss of stability

Total knee replacement (TKR) procedure is performed primarily to treat knee osteoarthritis (OA), a progressive condition hallmarked by a gradual degeneration and loss of articular cartilage. OA affects millions of Americans, with the knee the most commonly afflicted joint. Over 600,000 primary TKR surgeries are performed annually in the United States, which is predicted to increase to 3.48 million procedures in 2030 (Kurtz et al., 2007). OA accounts for over 95% of these surgeries (Mahomed et al., 2005). Other potential reasons for surgery include inflammatory arthritis, fracture, dysplasia, and malignancy (Ghosh and Chatterji, 2013; Guo et al., 2018). During the TKR procedure, the worn surfaces within the knee joint are replaced by artificial components/prosthesis, typically made of metal and/or hard plastic components with smooth articulating surfaces. There are three main components of an artificial knee joint – the femoral component, the tibial component and the patellar component (Figure 1-1).

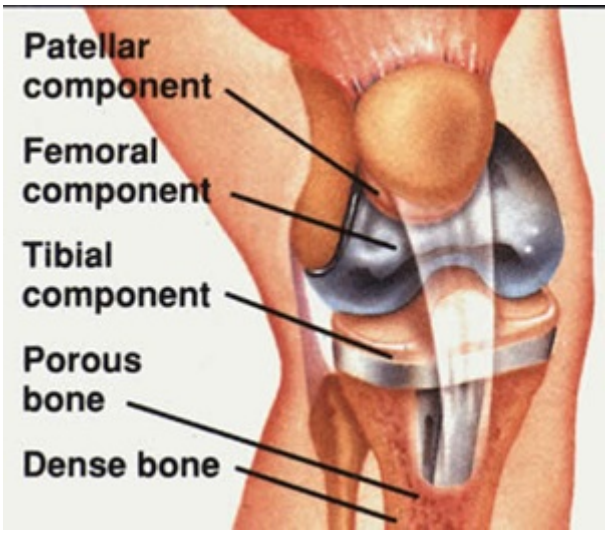

Figure 1-1. Total knee replacement components. Taken from "Knee Replacement Surgery," (n.d.)

Surgery begins with an incision being made over the front of the knee. Once the joint is exposed, the surgeon will loosen the surrounding muscles and ligaments and turn the patella out of its place. The worn surfaces within the joint, including the articular surface of the patella, are removed and the ends of the bones reshaped. The prosthesis components are attached to the bone ends using specialized bone cement and fitted together. The muscles and ligaments are repositioned and, if necessary, the ligaments are readjusted to achieve the best possible knee function.

Up to 25% of TKR patients remain dissatisfied with their surgical outcome (Dawson et al., 1998; Nam et al., 2014; Noble et al., 2005). Instability is a cause of dissatisfaction following TKR (Abulhasan and Grey, 2017; Bourne et al., 2010; Noble et al., 2005) and has been shown to be more significant during demanding activities (Davidson et al., 2013). Knee instability can be defined as an inability to maintain a single leg stance due to joint subluxation as a result of pathological laxity, or self reportedly as the sensation of buckling, shifting, or giving way of the knee (Felson et al., 2007). Knee instability is commonly used interchangeably with laxity, however laxity is

instead a clinical sign that is measured passively, and defined as excessive joint movement of the knee within the constraints of its ligaments (Abulhasan and Grey, 2017).

Knee stability is influenced by the articular geometry, ligament integrity, muscular contraction and kinetic loading conditions of the joint. A TKR procedure results in a joint without menisci and typically lacking one or both cruciate ligaments. The anterior cruciate ligament, which primarily resists anterior and rotational displacement of the tibia relative to the femur, is removed during surgery, whilst the posterior cruciate ligament, which prevents excessive posterior displacement of the tibia, may also be removed. Tension and integrity of other surrounding ligaments and tendons can also be altered during surgery, further compromising knee stability. Implants partially replace the function of these structures through intrinsic constraints, such as shapes of the articular surfaces, ligament substituting post/cam mechanisms, and guided motion of tibial bearings. However, no current implant design replicates the constraints of the healthy knee, and knee stability is thus potentially compromised.

Incidences of joint instability have been reported in TKR patients during high demand activities both through clinical observations and fluoroscopic evaluation (Daniilidis et al., 2012; Schwab et al., 2005; Waslewski et al., 1998). 32% of patients with self-reported knee instability prior to surgery continued to report instability six months post-surgery, with these patients found to have significantly greater knee pain and activity limitations (Fleeton et al., 2016). Anterior slide of the femur during knee flexion is commonly reported post-surgery (Banks et al., 2003b; Banks and Hodge, 2004; Delport, 2006; Dennis et al., 2003; Stiehl et al., 2003), which reduces tibiofemoral range

of motion and quadriceps moment arms and efficiency (Banks and Hodge, 2004; Dennis et al., 2003; Mahoney et al., 2002).

Muscle Activation Strategies in The Unstable Knee

During everyday activities, an unstable knee joint can result in altered activation of muscles surrounding the knee, particularly in the hamstrings, as well as medial quadriceps and gastrocnemius (Davidson et al., 2013; Lewek et al., 2005; Schmitt and Rudolph, 2008). Muscular co-contraction is commonly observed in patients, whereby opposing muscle groups contract simultaneously in response to instability (Figure 1-2).

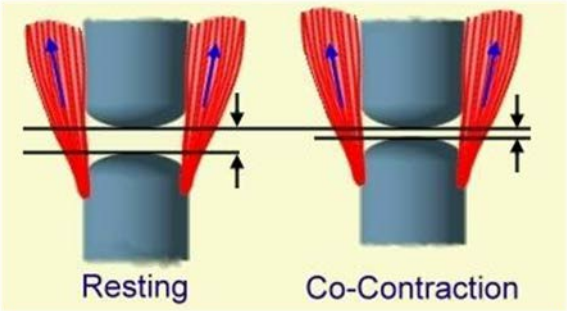

Figure 1-2. Muscular contraction response to knee instability. Taken from ("Musculature" n.d.)

During gait, patients with medial knee OA and corresponding instability exhibit greater medial knee muscular contraction in response to perturbations (Lewek et al., 2005), whilst post-surgical TKR patients have slowed gait, limited sagittal plane knee range of motion and knee extension moment, and prolonged muscular co-contractions during stance (Benedetti et al., 2003). For other activities of daily living, muscular co-contraction and altered movement strategies are also evident when knee instability is present. Reduced quadriceps muscle recruitment in the surgical limb was found for a sit-to-stand task in post-operative patients (Davidson et al., 2013). Altered muscle activation patterns have been shown to persist for a stair ascent and descent task and be more

significant as the demand of the activity increases (Severijns et al., 2016). Joint angle also plays a significant role in influencing knee instability and the muscle co-contraction response. At flexion angles greater than 30°, significantly great IE rotation and AP translation was observed at the knee joint in response to muscular co-contraction (Li et al., 2004).

Co-contraction of these muscles can compensate for joint instability and reduce tibial motion via increased compression across the joint (Biscarini et al., 2013; Imran and O'Connor, 1998; Li et al., 1999). However, muscular co-contraction can be mechanically inefficient and hinder joint functionality. Furthermore, the relative sliding of components and higher compressive load can lead to greater implant wear. More conforming implant designs that provide greater knee stabilization have been shown to have significantly lower wear rates (Brockett et al., 2017; Reinders et al., 2014).

Although these impairments in muscle activation and strength can be reduced with a targeted training program (Chmielewski et al., 2002; Petterson et al., 2009), such modifications are not routinely prescribed (Lingard et al., 2000). Furthermore, gait and muscular contraction abnormalities are still shown to be present even after extensive follow up treatment (Benedetti et al., 2003; Farquhar et al., 2008). It is therefore paramount that the implant can provide adequate stability to reduce the demands on the musculoskeletal system.

Methods of Characterizing Stability in The Natural and Implanted Knee

Various in vitro and in vivo mechanical tests have characterized the laxity of the natural knee. Laxity is measured passively, and it is presumed that excessive passive motion in the knee joint automatically leads to instability during dynamic and functional

activities (Schmitt et al., 2008). Excessive laxity in knee implants can be defined as a device that produces laxity that exceeds that of the natural knee (Walker and Zhou, 1987). Excessive prosthetic laxity leads to the risk of instability, soft tissue attenuation, edge-loading on components, and high contact stresses on the plastic. Inadequate prosthetic laxity may lead to altered kinematics and excessive stresses at the interface, running the risk of long-term loosening. Mechanical tests evaluate knee laxity based on motion in response to a cyclic anterior-posterior (AP) or internal-external (IE) force. Motion is dependent on knee flexion angle and the loads applied. A 100 N AP load and 5 Nm IE load have produced displacements ranging from 8 – 12 mm and 20 – 35°, respectively (Fukubayashi et al., 1982; Hsieh and Walker, 1976; Markolf et al., 1981, 1978; Wang and Walker, 1974). Similar tests have been performed on total knee replacements, typically in accordance with ISO or ASTM standards (Bartel et al., 2005; International Organization for Standardization., 2014; Klein et al., 2003; Moran et al., 2008; Walker and Zhou, 1987) whereby the TKR implant is mounted in a test machine and cyclic loads and torques are applied (Figure 1-3). Significant variation is seen in the displacement response, depending on the implant design (Walker and Haider, 2003). When tested in isolation, the laxity of the implant is quantified purely based on its mechanical constraint, providing an objective measure of its inherent laxity and stability that has the potential to improve the ability of surgeons to match the constraint needs of a patient with the constraint provided by specific implants. However, it should be recognized that such testing is performed in the absence of stabilizing soft tissue structures that are highly individualistic and dependent on surgical technique. In vitro tests overcome this limitation by incorporating natural structures of the knee that provide

greater constraint. Significant difference in knee laxity is seen with the inclusion of such structures. On average, soft tissue restraint was seen to reduce knee laxity by about 30% for lower conforming designs, whilst having little effect for higher conformities (Luger et al., 1997). Furthermore, under low compressive loads, knee dislocation was observed in the absence of soft tissue restraint (Luger et al., 1997).

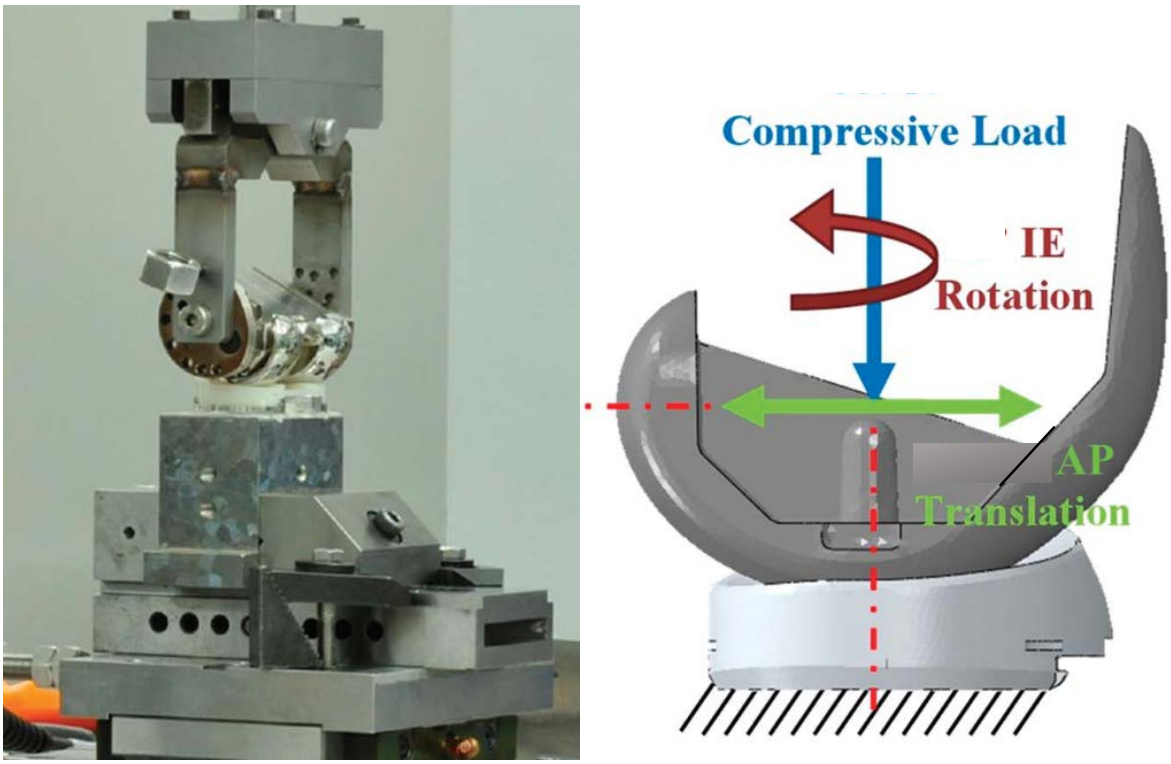

Figure 1-3. Mechanical evaluation of implant constraint. Taken from Rullkoetter et al. (2017)

Dynamic knee simulators have been used to evaluate implant laxity, incorporating natural stabilizing structures and attempting to reproduce the estimated kinematics and kinetics of the tibiofemoral (TF) and patellofemoral (PF) joints during dynamic activities. The range of motion, loading capability, control scheme, and simulation speed are just some of the characteristics that distinguish knee simulators from one another. The Kansas knee simulator has been employed to evaluate six degree-of-freedom (DOF) kinematics

of the TF and PF joints. With this electro- hydraulic mechanical design, a simulated femur and tibia independently flex and are attached to the ground through hip and ankle sleds (Figure 1-4). The resultant loads and kinematics of the knee are not controlled directly, and rather are reactions to the simulated quadriceps muscle and the applied external loads at the simulated hip and ankle (Maletsky and Hillberry, 2005).

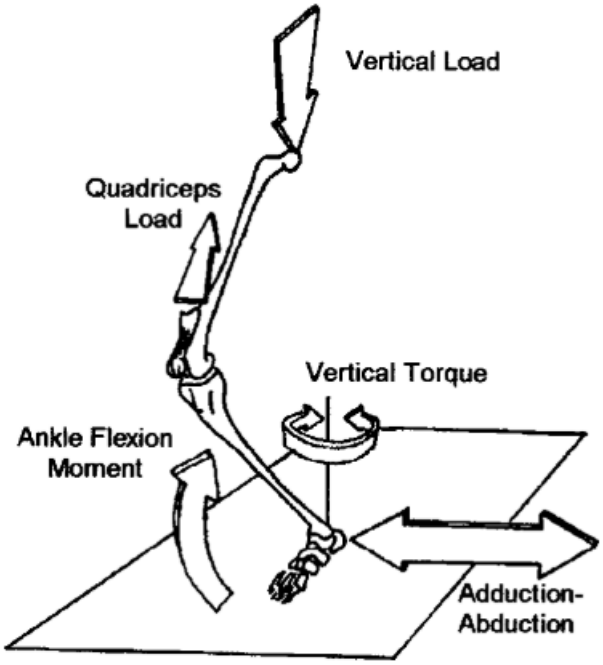

Figure 1-4. Kansas knee simulator design. Taken from Maletsky and Hillberry (2005)

The Stanmore simulator has been used to simultaneously evaluate kinematics and wear in the TF joint (Knight et al., 2007) and compare kinematics between different TKR designs (Desjardins et al., 2000). In this mechanical simulator, open loop controlled pneumatic force is used to simulate knee kinematics. A chamber containing the tibial component is mounted on the end of an actuator and articulates with the femur on a fixed flexion axis up to an angle of 58° (Asano, 2004) (Figure 1-5). One femoral flexion angle

waveform and three tibial force waveforms are delivered to the simulator to control the joints (Desjardins et al., 2000).

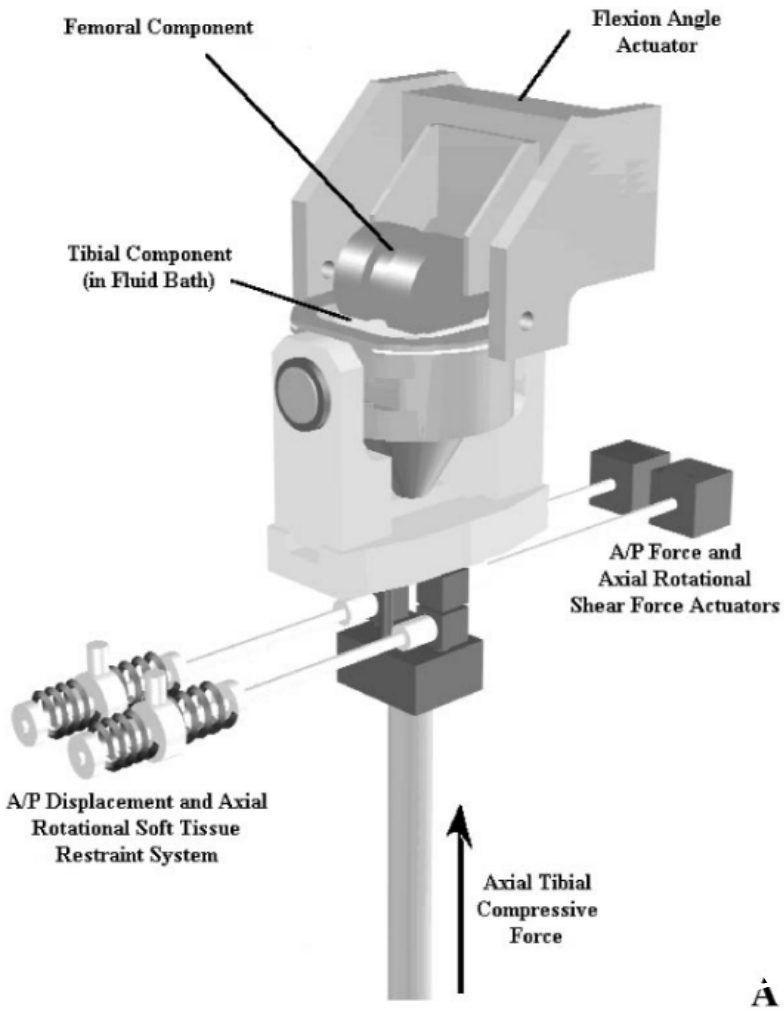

Figure 1-5. Stanmore knee simulator. Taken from Desjardins et al. (2000)

Even the most complex simulators have limitations in replicating in vivo loading conditions (Rullkoetter et al., 2017) and most simulators only replicate a simple knee bend motion (Verstraete and Victor, 2015). Furthermore, these test setups are typically unsuitable for the design phase of implant development, with evaluation of the implant geometry, alignment, or loading conditions generally being too time consuming, and production of implant prototypes costly. Validated computational models can be used to

quantify implant laxity in a more resource efficient manner. Computational testing of knee implants typically involves either finite element (FE) analysis or musculoskeletal (MS) multibody dynamics, or a combination of both.

A MS model consists of a skeleton with rigid body bony segments connected by joints and muscle-tendon units (Figure 1-6). This model allows computation of simple joint kinematics from full body motion capture, and inverse dynamics, with the function of each muscle analyzed by computing its length, moment arms, force and joint moments (Delp and Loan, 1995). OpenSim is an open source software frequently utilized for MS modelling. Inverse kinematics are computed by placing the model in a pose compatible with recorded experimental marker locations in each time step which are then compiled over the duration of the observed task. The kinematics solution is solved using a general quadratic programming solver, with a convergence criterion of 10^{-4} and a limit of 10^{3} iterations, that aims to minimize marker and coordinate error (Anderson et al., 2011). Accuracy of inverse kinematics can be quantified by RMS error, with maximum errors between experimental and model markers typically less than 2-4 cm, and RMS marker errors less than 2 cm (“Getting Started with Inverse Kinematics,” n.d.). Muscle forces are determined using inverse dynamics in conjunction with static optimization. With inverse dynamics, the generalized forces at each joint responsible for a given movement are computed. Static optimization then resolves the net joint moments into individual muscle forces at each instant in time, utilizing the accelerations from the inverse dynamics solution as a constraint whilst minimizing an objective function based on muscle properties.

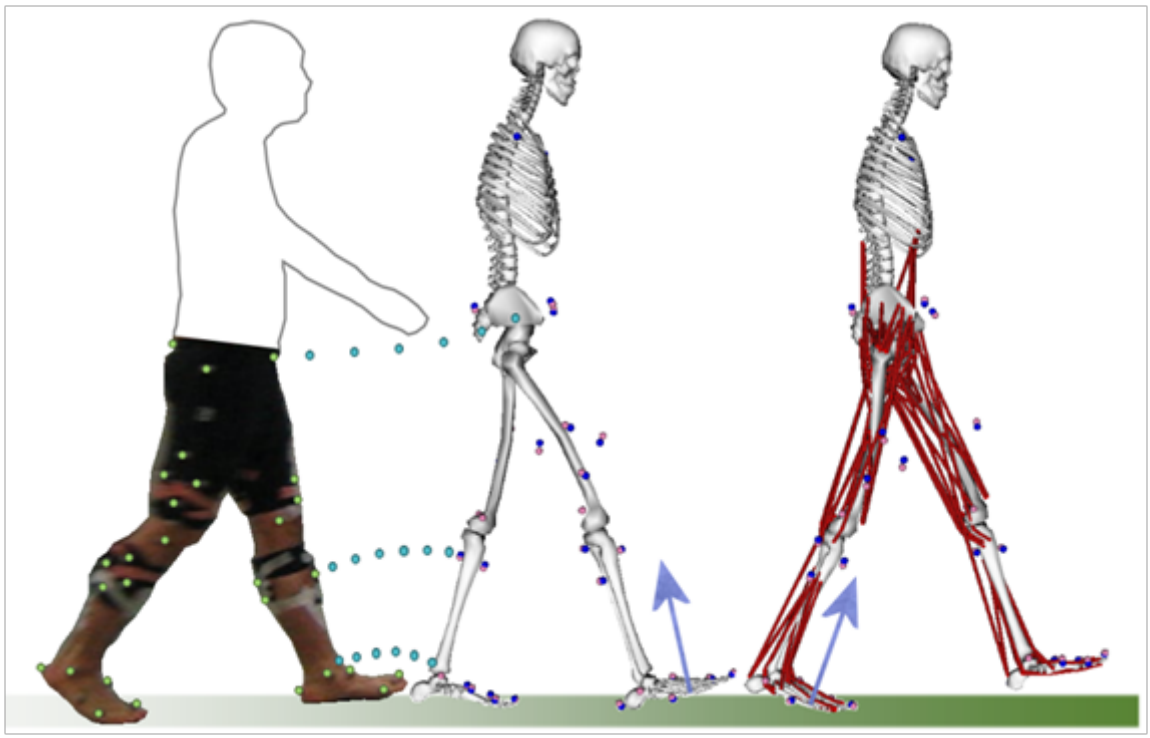

Figure 1-6. Full-body musculoskeletal modelling. Taken from Pronost and Sandholm, (n.d.)

A musculoskeletal modelling technique can consider the individual characteristics of the patients for biomechanical analysis and simulation, however, it does not provide detailed joint level analysis due to significant simplification. FE analysis is a type of numerical simulation whereby an object(s) are broken down into a number of finite elements, with mathematical equations used to predict the behavior of each element in response to loading and boundary conditions. The behavior of each object is then determined as an approximation to the solution of the sum of these equations by minimizing an associated error function. FE is used in orthopedic research to provide quantitative data on structural and mechanical variables using musculoskeletal experimentation (Kluess et al., 2010). FE simulations are commonly utilized at the joint scale, in order to predict local joint mechanics for a given prosthesis, or comparative analyses of joint mechanics for a variety of prostheses (Baldwin et al., 2012; Clary et al.,

2013; Halloran et al., 2005; Liau et al., 2002). FE models are frequently developed from and verified with dynamic knee simulators (Figure 1-7) and evaluate the mechanics of a set of components under limited static or standardized loading conditions, not accounting for dynamic and individualized muscular contraction. Furthermore, simulations usually involve only a single gait cycle or deep knee bend with optimal implant alignment (Baldwin et al., 2012; Desjardins et al., 2000; Kenawey et al., 2011; Kessler et al., 2009).

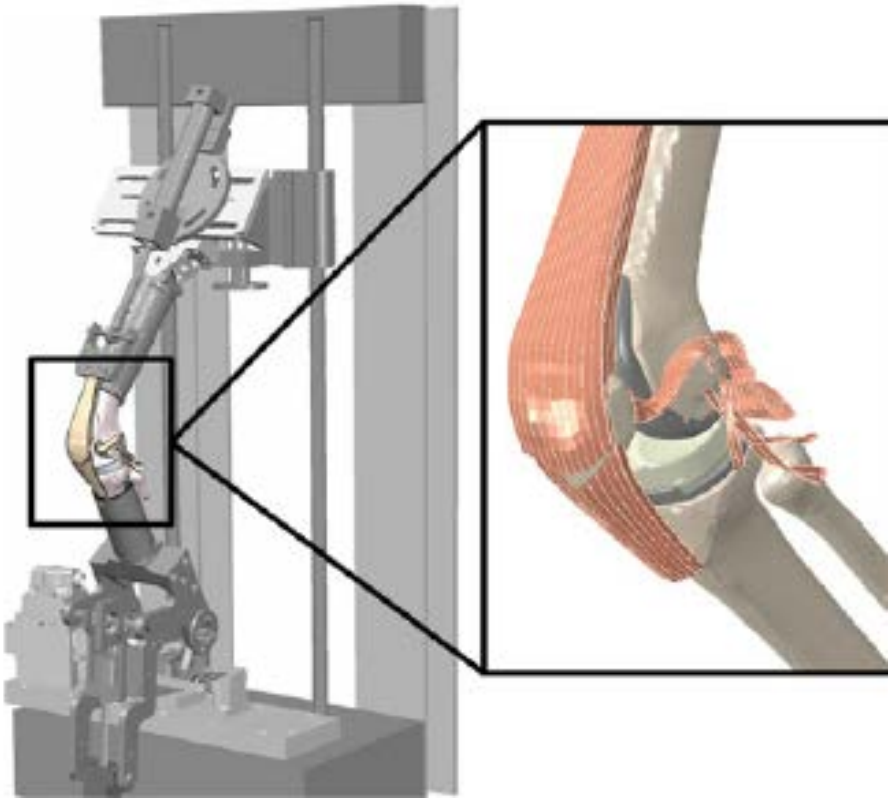

Figure 1-7. Finite element analysis of a dynamic knee simulator. Taken from Clary et al. (2013)

Implant Conformity and The Effect On Knee Stability

Implant testing has shown that a key influence on the laxity of an implant design is the level of conformity between the tibial tray and femoral component. In laxity testing using mechanical simulators, low conforming implants require greater soft tissue

constraint and dislocate under low compressive loads when compared to more conforming designs (Luger et al., 1997). Furthermore, TKR patients with low conforming designs providing less constraint have been shown to have greater incidence of muscular co-contraction (Rullkoetter et al., 2017). The implant conformity ratio, defined as the ratio of the radii of the femoral component to that of the tibial tray, can be used to quantify implant conformity. Current commercially available knee implant designs (PFC Sigma®, Attune®, Nexgen® and Triathlon®) have conformity ratios ranging from 0.22 to 0.88 (Sintini et al., 2018).

1.2 Motivation

Current methods for joint laxity evaluation typically do not account for the adaptive muscle response that occurs in vivo in response to knee instability. It should be recognized that proprioception factors and the central nervous system play a key role in the dynamic response of the patient to knee instability. Furthermore, most simulations only assess implant designs under ideal or simplistic loading conditions. To improve pre-clinical implant design evaluation, a spectrum of loading conditions, reflective of in vivo performance, should be investigated.

Computational simulations have the potential to accurately model the muscle adaptive response with change in implant design without requiring manufacture of physical prototypes. Validated, patient specific models can also provide insight into measures not easily obtained experimentally, such as muscle force requirements during a dynamic activity. Combining a full-scale MS model with a FE model allows for a detailed analysis of joint-level kinematics, forces, and contact mechanics and can

overcome the limitations of joint simplification of a full body MS model and the lack of patient kinetic and kinematic specificity of a FE model.

1.3 Research goals

This research aimed to establish the relationship between musculoskeletal adaptation patterns and joint stability by quantitatively evaluating the muscle force requirements required to maintain a consistent level of joint stability with changes in implant conformity. Presently, it is difficult to interpret how observed differences in implant motion directly impact patient muscle function and recruitment, and the ability to predict how the musculoskeletal system adapts to changes in knee stability is largely unknown. The overall objective of this thesis was to fill this gap in current knowledge, by investigating the effects of knee implant conformity on joint stability, utilizing a method that accounts for the muscle force requirements necessary to prevent excessive joint motion during dynamic activities.

A FE approach utilizing a patient specific, full body model has been utilized to efficiently evaluate different implant designs at key loading points during a variety of daily activities. The results may aid in understanding how surgical decisions regarding implant design affect functional outcomes for an individual undergoing TKR. Furthermore, the outcome of this study could serve to guide the clinician on the optimal choice of implant design based on the current and potential recovery of muscle strength of the patient.

CHAPTER TWO : MANUSCRIPT “THE EFFECT OF IMPLANT CONFORMITY ON MUSCLE FORCE REQUIREMENTS IN THE IMPLANTED KNEE"

2.1 Introduction

Total knee replacement (TKR) procedure is performed primarily to treat knee osteoarthritis, which accounts for 97% of TKR surgeries. Despite improvements in pain and functional limitations following surgery, up to 25% of patients remain dissatisfied with the surgical outcome (Dawson et al., 1998; Nam et al., 2014; Noble et al., 2005). Instability is a cause of dissatisfaction following TKR (Abulhasan and Grey, 2017; Bourne et al., 2010; Noble et al., 2005) and has been shown to be more significant during demanding activities (Davidson et al., 2013). Knee stability is influenced by the articular geometry, ligament integrity, muscular contraction and kinetic loading conditions of the joint. During a TKR procedure, internal stabilizing structures are altered, potentially compromising knee stability (Daniilidis et al., 2012; Schwab et al., 2005; Waslewski et al., 1998). Anterior slide of the femur during knee flexion is commonly reported post-surgery (Banks et al., 2003b; Banks and Hodge, 2004; Delport, 2006; Dennis et al., 2003; Stiehl et al., 2003) reducing tibiofemoral range of motion and quadriceps moment arms and efficiency (Banks and Hodge, 2004; Dennis et al., 2003; Mahoney et al., 2002).

During everyday activities, an unstable knee joint can result in altered activation of muscles surrounding the knee (Davidson et al., 2013; Lewek et al., 2005; Schmitt and Rudolph, 2008). Co-contraction of these muscles can compensate for joint instability and reduce tibial motion via increased compression across the joint (Biscarini et al., 2013;

Imran and O'Connor, 1998; Li et al., 1999). However, muscular co-contraction can be mechanically inefficient and can hinder joint functionality. Furthermore, the relative sliding of components and higher compressive load can lead to greater implant wear (Brockett et al., 2017; Reinders et al., 2014). TKR patients present with slowed gait, reduced range of motion and prolonged muscular co-contractions during stance (Benedetti et al., 2003). For other activities of daily living such as stair ascent/descent or sit to stand movements, co-contraction and altered movement strategies is evident (Davidson et al., 2013; Severijns et al., 2016) and more significant with demanding activities (Severijns et al., 2016).

Various in vitro and in vivo mechanical tests have characterized the laxity of the natural knee, evaluating stability based on motion in response to a cyclic anterior-posterior (AP) or internal-external (IE) force. Motion is dependent on knee flexion angle and the loads applied. A 100 N AP load and 5 Nm IE load have produced displacements ranging from 8 – 12 mm and 20 – 35°, respectively (Fukubayashi et al., 1982; Hsieh and Walker, 1976; Markolf et al., 1981, 1978; Wang and Walker, 1974). Similar tests have been performed on total knee replacement implants, typically in accordance with ISO 142243 (International Organization for Standardization., 2014; Klein et al., 2003; Moran et al., 2008; Walker and Zhou, 1987). When tested in isolation, the laxity of the implant is quantified purely based on its mechanical constraint, providing an objective measure of its inherent laxity and stability. Significant variation is seen in the displacement response, depending on the implant design (Walker and Haider, 2003). In vitro tests incorporate natural structures of the knee that provide greater constraint, and have been found to

reduce laxity by approximately one-third for lower conforming designs, whilst having little effect for highly conforming designs (Walker and Haider, 2003).

Dynamic knee simulators such as the Kansas knee simulator (Maletsky and Hillberry, 2005), and Stanmore simulator (Knight et al., 2007) have been used to evaluate laxity, incorporating natural stabilizing structures and attempting to reproduce the estimated kinematics and kinetics of the patellofemoral and tibiofemoral joints during dynamic activities. Even the most complex simulators have limitations in replicating in vivo loading conditions (Rullkoetter et al., 2017) and most simulators only replicate a simple knee bend motion (Verstraete and Victor, 2015).

Validated computational models can be used to quantify implant laxity in a more resource-efficient manner. Computational testing of knee implants typically involves either finite element (FE) analysis or musculoskeletal (MS) multibody dynamics. FE simulations are commonly utilized at the joint scale, in order to predict local joint mechanics for a given prosthesis, or comparative analyses of joint mechanics for a variety of prostheses (Shu et al., 2018). However, these methods for joint laxity evaluation typically do not account for the adaptive muscle response that occurs in vivo in response to knee instability. It is difficult to interpret how the observed differences in implant motion directly impact patient muscle function and recruitment. Consequentially, the ability to predict how the musculoskeletal system adapts to changes in knee stability is largely unknown. This research investigated the effects of knee implant conformity on joint stability, via a method that accounts for the muscle force requirements necessary to prevent excessive joint motion during dynamic activities. The overall goal is to establish a relationship between musculoskeletal adaptation patterns and joint stability by

objectively quantifying the muscle force requirements required to maintain a consistent level of joint stability with changes in implant conformity.

2.2 Material and methods

Lower Extremity Opensim Modeling

Using the rigid-body musculoskeletal modeling software, OpenSim (Delp et al., 2007), joint kinematics and muscular loads were extracted at key instances in daily activities. Daily activities consisted of walking up and down stairs, a lunge, normal gait and a step up task, all completed on the implanted leg. For the lunge activity, the instances of interest were heel-strike, toe-off, and the peak tibiofemoral flexion angle. For the other activities, instances were heel-strike, toe-off, and the first and last peak in vertical ground reaction force as shown in Figure 2-1. These time points were chosen to subject the knee joint to the kinematic and loading conditions most likely to cause instability due to abrupt changes in loading.

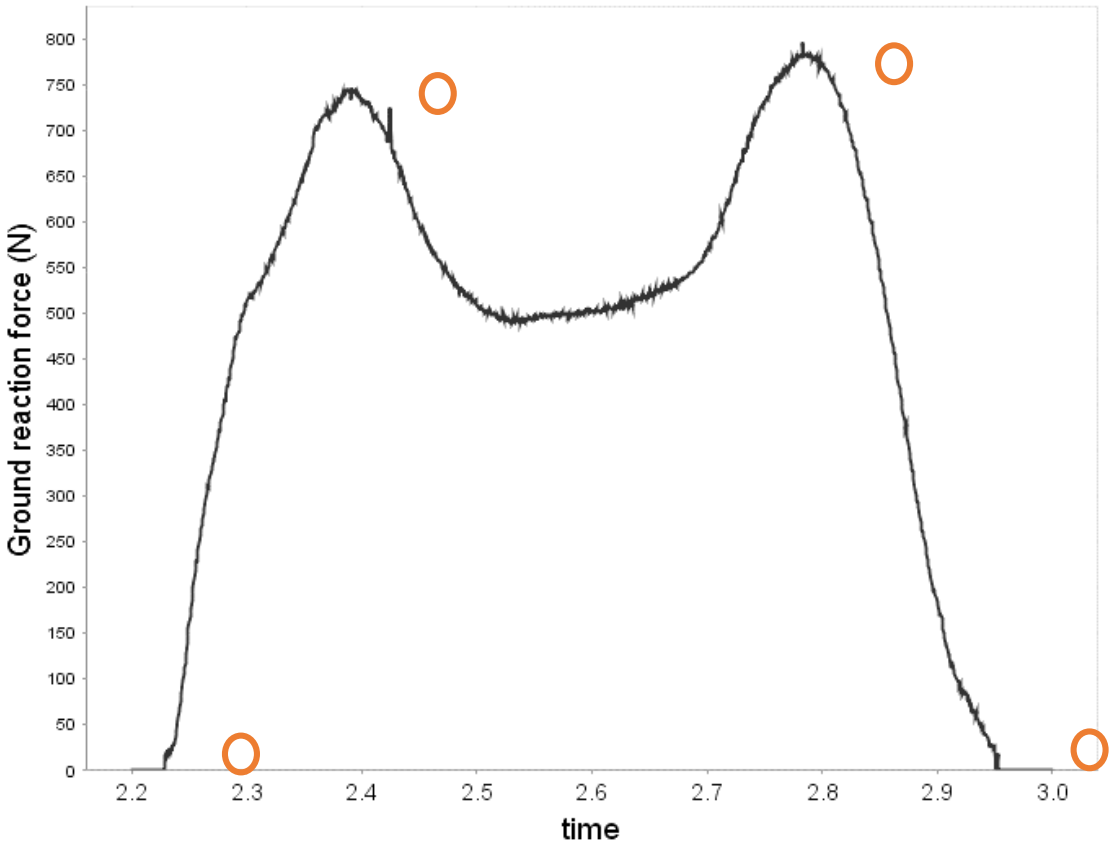

Figure 2-1. Force time plot showing key time instances examined -indicated by red circles.

The OpenSim model, provided with the Grand Challenge dataset, consisted of the right lower limb with nine rigid body segments defined by CT scan geometry, 44 musculotendon actuators, and 24 DOF (Figure 2-2). Muscles were modelled using a Hill-type model (Schutte et al., 1993). Joint angles and translations extracted from the rigid-body musculoskeletal simulations were converted to a Grood and Suntay joint coordinate system (Grood and Suntay, 1983). Muscle forces were predicted using static optimization to resolve the net joint moments into individual muscle forces at each instant in time (Ackermann, 2007; Delp et al., 2007).

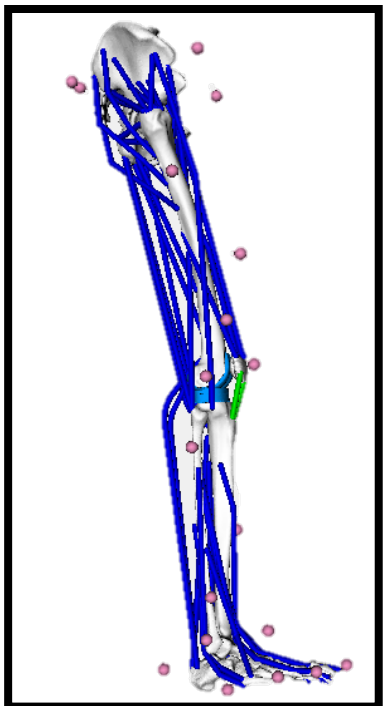

Figure 2-2. OpenSim musculoskeletal model of the lower leg

Experimental Data

Marker-based whole-body motion capture, ground reaction force, and computed tomography (CT) imaging data were sourced from the Fourth Grand Challenge Competition data set for predicting in vivo knee loads (Lloyd et al., 2013). The test subject was male, age 83 years, height 166 cm, and body weight (BW) 64.6 kg, with a PFC Sigma (DePuy Synthes) right knee replacement. Five activities of daily living were examined: over ground walking, lunge, walking up and down stairs, and a step-up onto a box.

Finite Element Model

The FE model included subject-specific bone geometry from patient CT data. Bones were defined as rigid bodies with an average element edge length of 5mm, and mass and inertial properties consistent with the OpenSim model. Ligaments, modelled as two dimensional reinforced membrane elements, consisted of the patella tendon (PT),

medial and lateral patellofemoral ligaments (MPFL, LPFL), lateral collateral and popliteofibular ligaments (LCL, PFL), anterior lateral capsule (ALC), superficial medial collateral ligament (sMCL), anterior-lateral and posterior-medial bundles of the PCL (alPCL, pmPCL), and medial and lateral posterior capsules (PCAPL, PCAPM) (Baldwin et al., 2012; Harris et al., 2016). Implant components were defined as rigid bodies, with a pressure overclosure contact relationship and friction and damping coeffcients of 0.01. A set of 40 lower body muscles, consistent with those utilized in the OpenSim model, were modelled as axial connectors, with the rectus femoris and three vastii muscles modelled as reinforced truss connectors to allow for muscle wrapping with knee flexion. The coordinate of each muscle attachment point was obtained from the OpenSim model (Delp et al., 2007). Loads were applied to axial connectors to simulate muscle forces along corresponding lines of action. (Figure 2-3)

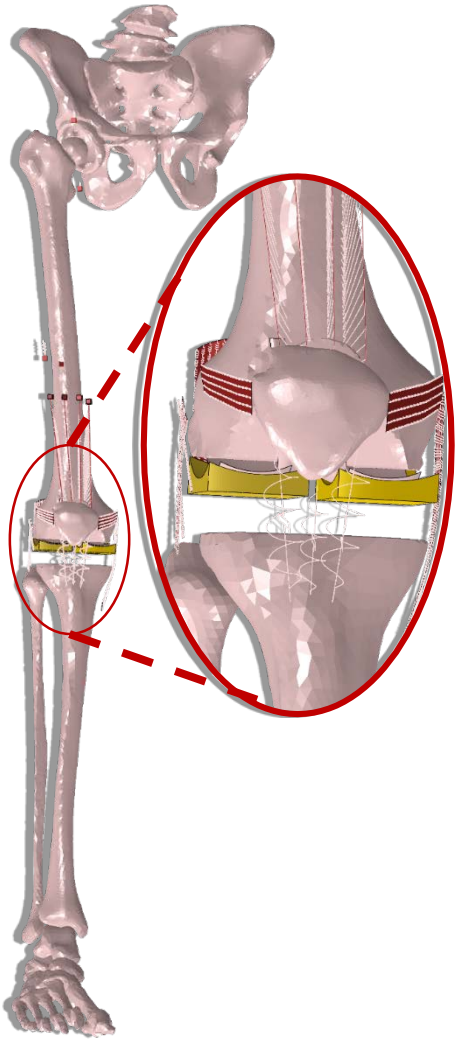

Figure 2-3. Finite Element model of the lower leg

Simulations were performed with the patient's implant geometry, in addition to a series of computationally-generated implants with conformity ratios (CR) between the femoral and tibial components which varied from 0.1 to 0.6. Conformity was quantified by the ratio between the distal femoral and tibial insert radii. In each case, the same computationally-generated femoral component was used in combination with a variety of tibial inserts (Figure 2-4). The range of conformities utlitilzed were chosen to be of comparable range to implant designs in the current market (Sintini et al., 2018). The upper limit of 0.6 was set to be consistent with the patient implant confomity ratio, which

would provide a baseline geometry for comparision. A higher range was not included as a level of conformity greater than 0.6 was too constrained to match a desired target level of implant motion.

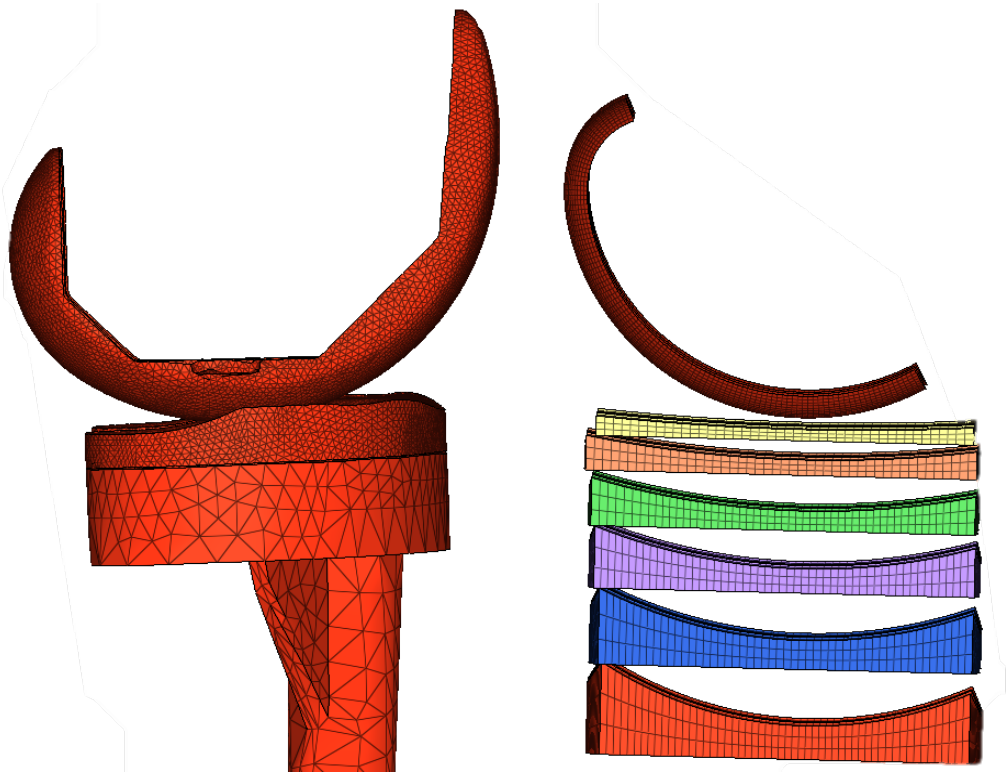

Figure 2-4. Patient (left) and generated (right) implant geometries showing different levels of conformity

Laxity Testing

The dynamic, subject-specific FE model was implemented in Abaqus/Explicit ("Abaqus 6.14 Online Documentation," 2013). All five activities were simulated and, for each key instance in each activity, tibiofemoral laxity was quantified. Muscle loads, ground reaction forces and hip and ankle joint kinematics at that instance were applied to the model prior to beginning the laxity tests. Tibiofemoral flexion was kinematically prescribed, but all other DOF at the knee were unconstrained to allow the joint to settle into a neutral position. Ground reaction forces and all muscle loads were held constant

over the duration of the laxity test. The most conforming implant, (CR = 0.6) was initially virtually implanted into the FE model. A series of laxity tests were performed whereby a ramped external load of ± 500 N or ± 20 Nm was applied to the knee joint to induce either AP translation or IE rotation, respectively. The result was four distinct laxity tests that simulated ISO implant testing, with AP and IE directionality set to describe the motion of the tibia relative to the femur. The resulting joint kinematics were extracted and used as the "target" AP or IE kinematic profile for each instance within each activity.

This series of laxity tests was subsequently repeated for each of the other sets of implants, however, in these simulations, muscle forces for a subset of thirteen muscles were not prescribed in advance. Instead, the muscle activation response necessary to achieve the target AP or IE kinematic profile was determined using proportional–integral (PI) control. The controlled muscles depended on the direction of the laxity test and were selected based on whether their contraction would resist displacement due to the applied load. The rectus femoris, vastus medialis, vastus intermedius and vastus lateralis were controlled for the posterior test, whilst the semimembranosus, semitendinosus, sartorius, biceps femoris (short and long head), gracilis, tensor fasciae latae and gastrocnemius (medial and lateral) were those included for the anterior test. For the internal test, the rectus femoris, vastus medialis, vastus intermedius and vastus lateralis, lateral gastrocnemius, biceps femoris (short and long head) and tensor fasciae latae were selected, whilst the external test controlled the rectus femoris, vastus medialis, vastus intermedius, vastus lateralis, medial gastrocnemius, semimembranosus, semitendinosus, sartorius and gracilis. The muscle loads determined from the OpenSim inverse dynamics

were applied as the starting value for PI control. During the laxity simulations, the forces applied to the controlled muscles were free to vary, with the force distribution amongst these muscles held constant during the laxity test at the ratios determined from the OpenSim simulations. A sensor in the FE model monitored either the AP translation or IE rotation of the knee joint in relation to the target kinematic profile for each increment in the analysis (Figure 2-5). The PI controller calculated the muscle force output required for the sensor to match this target profile; this muscle force was then applied in the subsequent increment. The controller interfaced with the FE model through an Abaqus/Explicit user subroutine, coded in the Fortran language. The muscle force requirements for each set of implants were compared across activities and laxity tests.

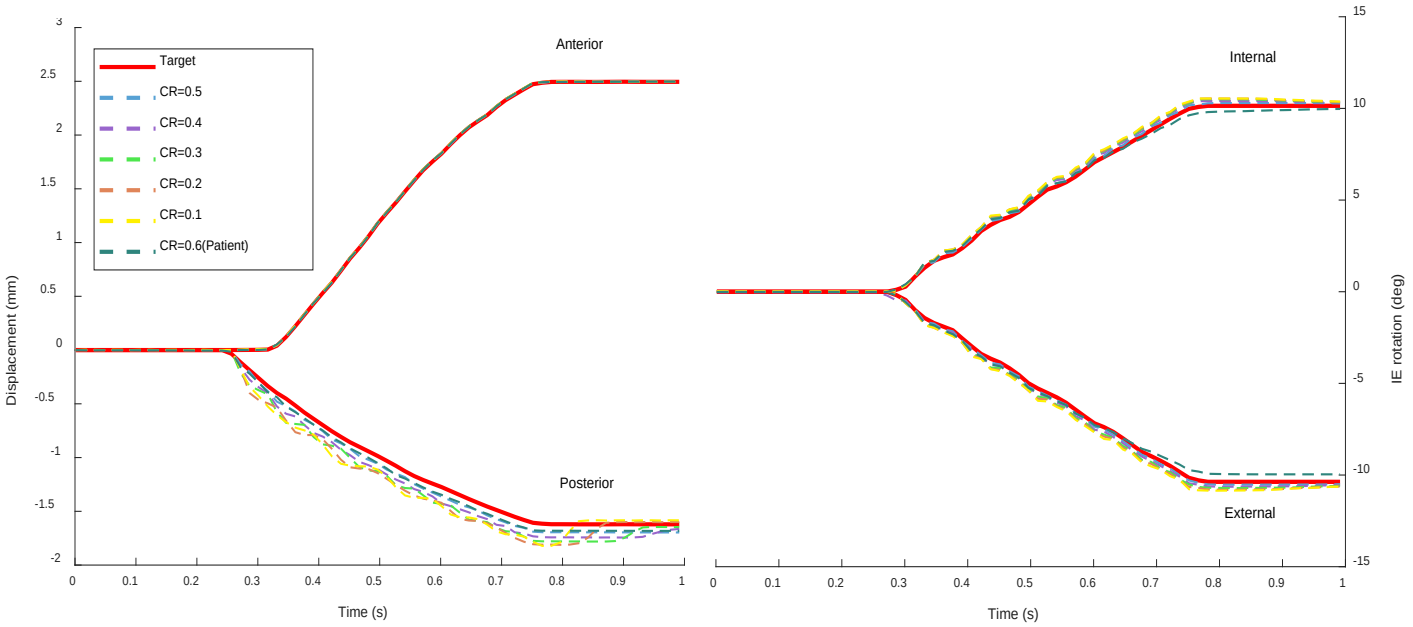

Figure 2-5. Target and achieved kinematic profiles for all laxity test directions, showing implant conformity ratios (CR)

Model Verification

To verify the accuracy of the PI controller in determining the muscles forces to achieve the target kinematic profile, the root mean square (RMS) error between the target

and measured positions was computed at the conclusion of each laxity test for each level of implant conformity.

To examine the accuracy of the FE model in replicating the knee motion of the patient, the RMS error of the unconstrained knee joint kinematics at each activity instance between the Grand Challenge fluroscopic data and the generated and patient implants were compared.

Statistical Analysis

The primary dependent variable for this study was normalized muscle force, whereby for each laxity test, the PI controlled total muscle force was normalized to the force required for the implant with the lowest conformity (CR = 0.1), which was typically the level of conformity requiring the greatest force. Other dependent variables examined were tibiofemoral and patellofemoral joint contact area and pressure, and tibiofemoral joint axial load. The two independent variables were conformity ratio and activity type.

Data was categorized by activity, loading direction (rotational/IE and translational/AP) and conformity level. For each dependent variable, 2-way multivariate analysis of variance (ANOVA) ($p < 0.05$) was employed to test the main effect of the factors of conformity level and activity type on the mean. If conformity was determined to be a main effect, multiple pairwise comparisons were utilized to test whether there existed significant differences between each independent variable grouping when compared to the patient geometry and least conforming (CR = 0.1) implant geometries. A Bonferroni correction method was used to adjust for type I errors, with critical values obtained from Student's t-distribution. ("Multiple comparison test," n.d.)

A regression analysis was completed for each activity type and loading direction (AP or IE) data grouping. The correlation between the level of conformity and each dependent variable was determined using a MATLAB program that fitted a linear regression model to the data. R-squared values were computed to indicate goodness of fit.

2.3 Results

Model Verification

RMS error between the final target and achieved displacements for AP tests was less than 0.12 mm for the generated geometries and equal to 0.20 mm for the patient implant. For the IE tests, RMS rotational errors were less than 0.37° across all implant geometries (Table 2-1).

Table 2-1. RMS error between target and achieved kinematics for each level of implant conformity using PI muscle force control

	RMS ERROR	
CONFORMITY	**AP TRANSLATION (MM)**	**IE ROTATION (DEG)**
0.1	0.080	0.202
0.2	0.117	0.266
0.3	0.131	0.330
0.4	0.118	0.352
0.5	0.115	0.303
0.6 (PATIENT)	0.201	0.368

Comparison of the patient implant with recorded fluoroscopic kinematics produced RMS errors of 0.8° and 4.1° for varus-valgus (VV) and IE rotations, respectively (Table 2-2). For IE rotation, this variation is up to 50% of the total range of motion observed during laxity testing, with target rotations typically between 8-10°. RMS errors for AP and ML translation between the patient implant and recorded fluoroscopic kinematics were 1.2 mm and 0.4 mm respectively (Table 2-2). With target kinematic

displacements ranging between approximately 4-5mm for AP directed tests, AP variation was approximately 25% of the total range of motion.

Table 2-2. RMS error (+/- STD) comparing patient implant model with fluoroscopic measures of tibiofemoral kinematics

RMS ERROR	VV ANGLE (DEG)	IE ANGLE (DEG)	AP TRANSLATION (MM)	ML TRANSLATION (MM)
PATIENT	0.799 +/- 0.567	4.09 +/- 2.14	1.16 +/- 0.785	0.396 +/- 0.562

Normalized Muscle Force

Regression analysis for normalized muscle force and implant conformity was performed for each activity and load direction. Overall, as the conformity of the implant increased, a decrease in the muscle force required was evident. On average, as implant conformity increased by 0.1, muscle force requirements were reduced by 10.4%. For AP directed loading tests, similar correlations were seen across activities, with the stair down activity showing the strongest correlation (R^2=0.83), whilst other activities had R^2 values ranging from 0.65 to 0.76 (Figure 2-6). For the IE loading direction, the gait activity had the lowest R-squared value (R^2=0.17), whilst the stair down activity showed the strongest

correlation (R^2=0.91). The lunge, stair-up and step-up activities had R-squared values of 0.68 0.68, 0.54, and 0.68 respectively.

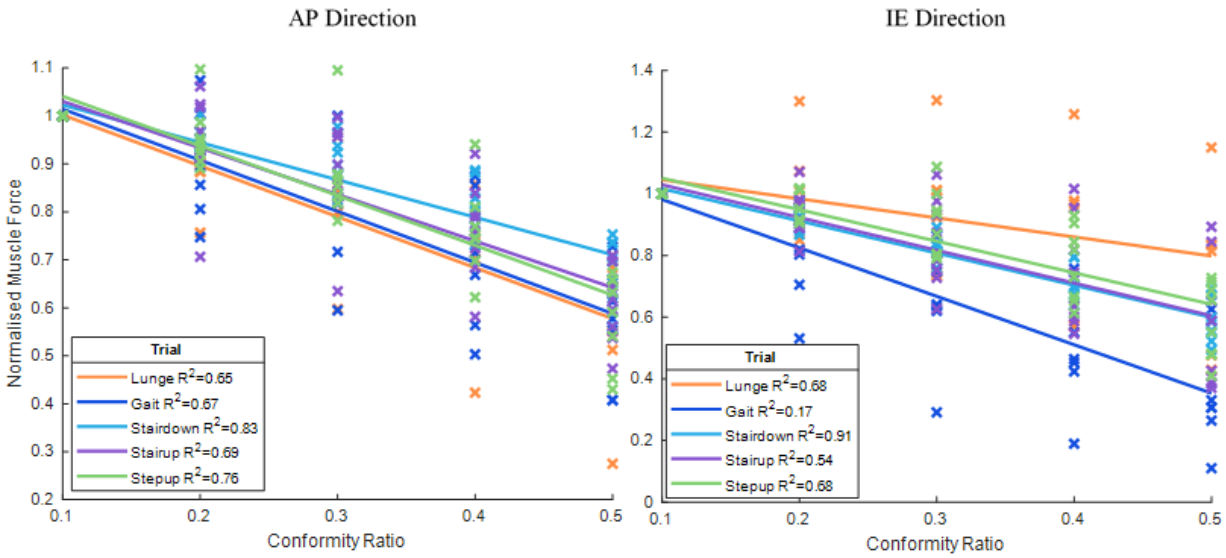

Figure 2-6. Normalized muscle force regression analysis across all activities, showing AP and IE loading directions

When compared to the least conforming implant (CR = 0.1), conformities of 0.5, 0.4 and 0.3 saw significantly lower normalized muscle force requirements across all activity types. Apart from the implant with CR=0.5, implants were seen to have significantly different normalized muscle force from the patient implant (Figure 2-7).

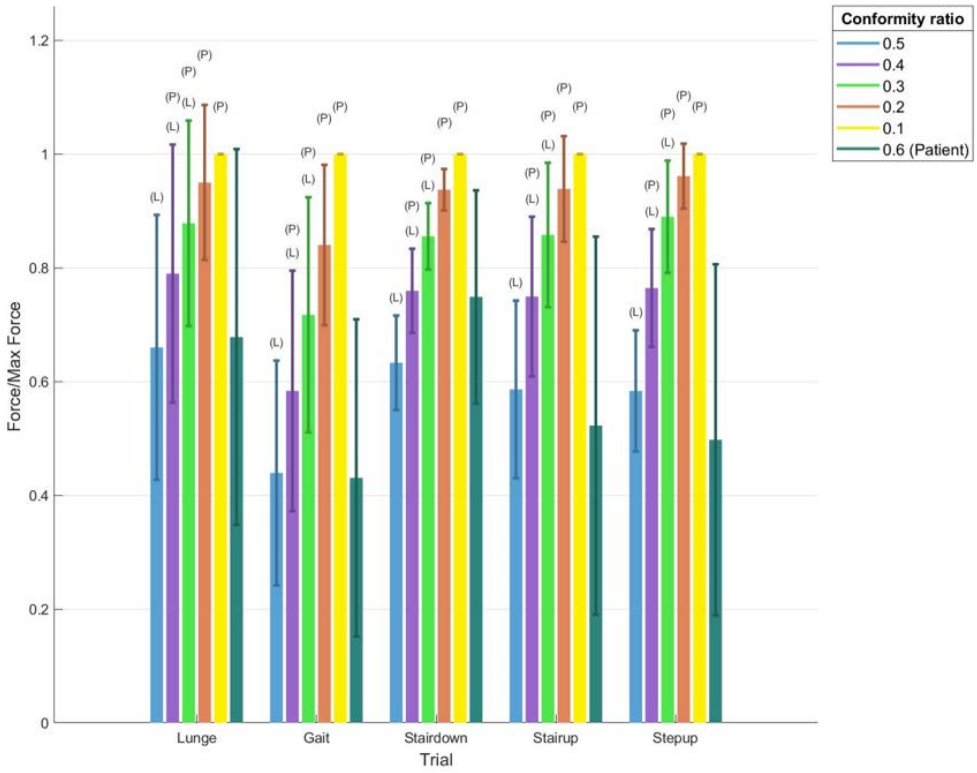

Figure 2-7. Normalized muscle force comparison for each trial type showing mean and standard deviation. (P), (L) indicates significant difference (P<0.05) from patient implant and least conforming (CR=0.1) implants respectively

Contact Area

Regression analysis between tibiofemoral joint contact area and conformity ratio showed tibiofemoral contact area to decrease with decreasing conformity. A stronger correlation was observed for AP directed loading tests when compared to IE directed tests (Figure 2-8). The gait task showed little correlation for both testing directions. Stronger correlations were found in the lunge and stairdown activity for AP directed tests

(R^2=0.71 and 0.68 respectively), with the strongest correlation seen in the step-up activity for the IE directed tests (R^2=0.58).

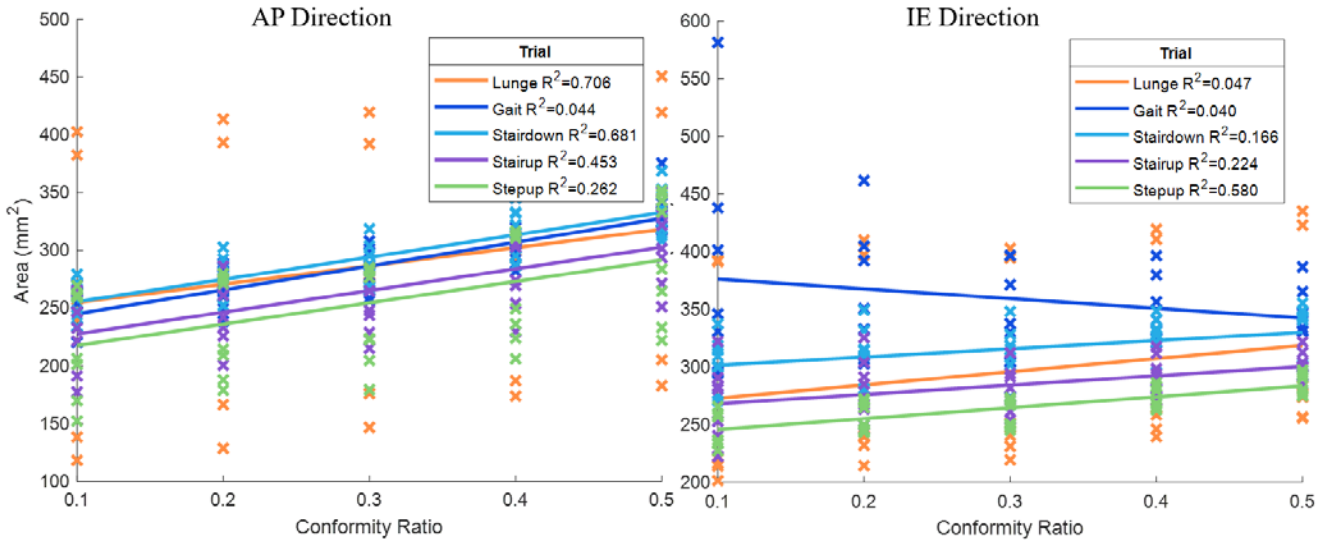

Figure 2-8. Tibiofemoral joint contact area regression analysis across all activities, showing AP and IE loading directions

For the ANOVA comparison, aside from the gait activity which showed no observable trend, tibiofemoral contact area decreased with decreasing conformity (Figure 2-9). This difference was only statistically significant when comparing the highest and lowest implant conformities. All generated implants were seen to have significant difference in tibiofemoral contact area from the patient implant.

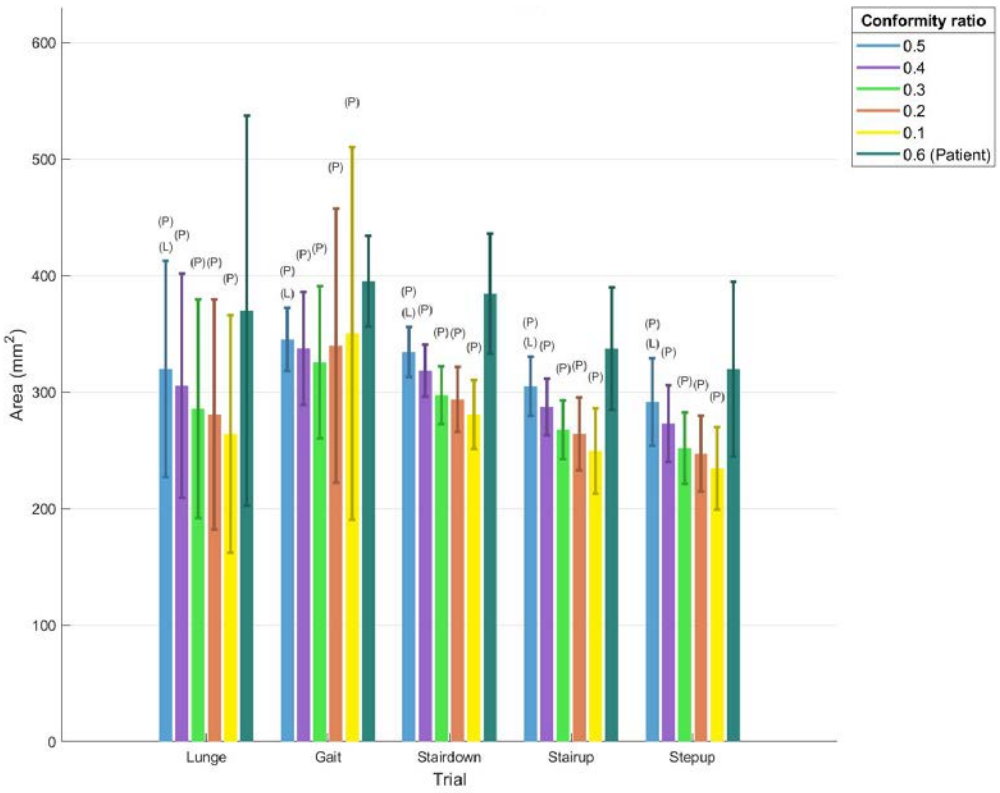

Figure 2-9. Tibiofemoral joint contact area for each trial type showing mean and standard deviation. (P), (L) indicates significant difference (P<0.05) from patient implant and least conforming (CR=0.1) implants respectively.

Regression analysis between patellofemoral joint contact area and conformity ratio showed patellofemoral contact area to increase with decreasing conformity. As illustrated in figure 2-10, the strength of the correlation varied between activities and loading direction. In general, stronger correlations were observed for IE directed loading tests when compared to AP directed tests. Overall, R-squared values were relatively low, with the highest values seen in the lunge, step-up and stairdown activities for the IE directed tests (R^2=0.60, 0.59 and 0.37 respectively) and all other R-squared values below 0.3.

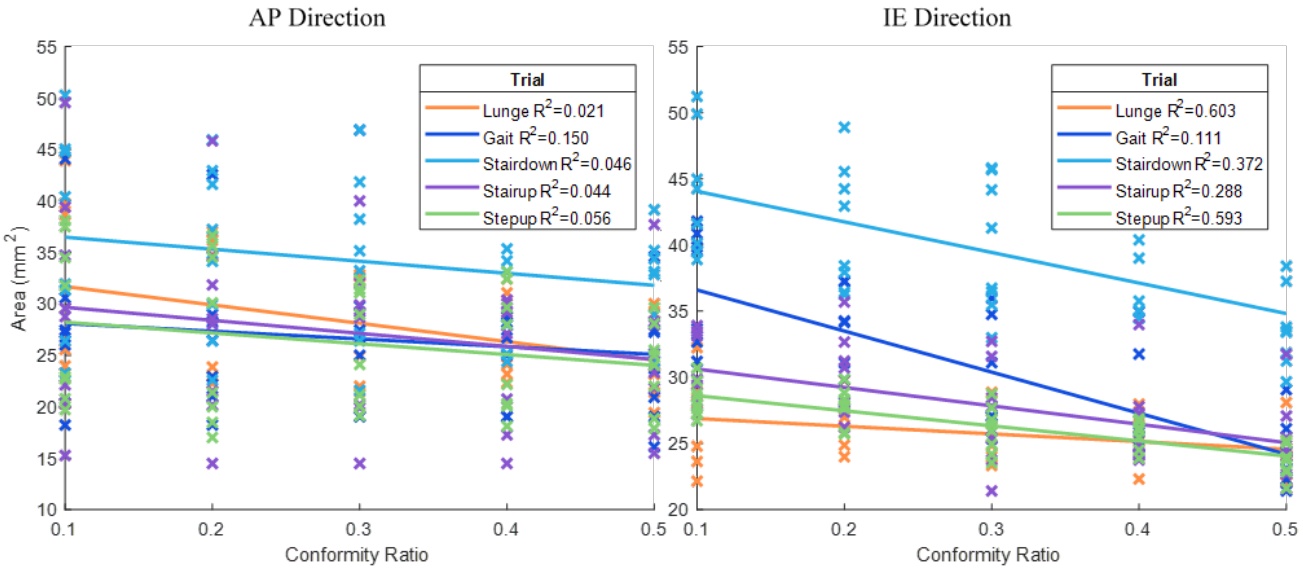

Figure 2-10. Patellofemoral joint contact area regression analysis across all activities, showing AP and IE loading directions

For the ANOVA comparison, patellofemoral contact area increased with decreasing implant conformity, however the difference was not statistically significant. Significantly higher patellofemoral contact area was found for the patient implant when compared to the generated implants (Figure 2-11).

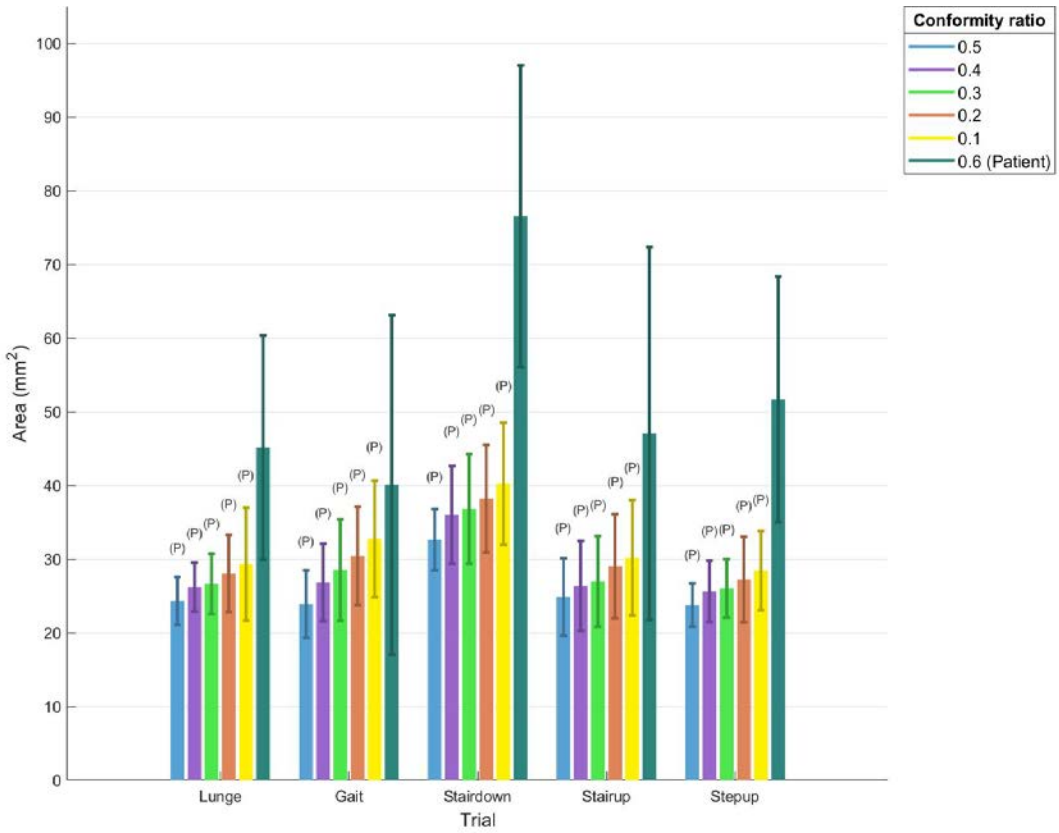

Figure 2-11. Patellofemoral contact area comparison for each trial type showing mean and standard deviation. (P) indicates significant difference (P<0.05) from patient implant

Contact Pressure

Regression analysis between tibiofemoral joint contact pressure and conformity ratio showed tibiofemoral contact pressure to increase with decreasing conformity, with the strength of the correlation varying across activities and loading directions (Figure 2-12). Apart from the gait activity, stronger correlations were seen in IE directed tests, with R-squared values above 0.6. For AP directed tests, the strongest correlations were

observed across lunge and stairdown activities (R^2=0.50 and 0.62 respectively), with other activities showing a weak correlation, with R-squared values less than 0.1.

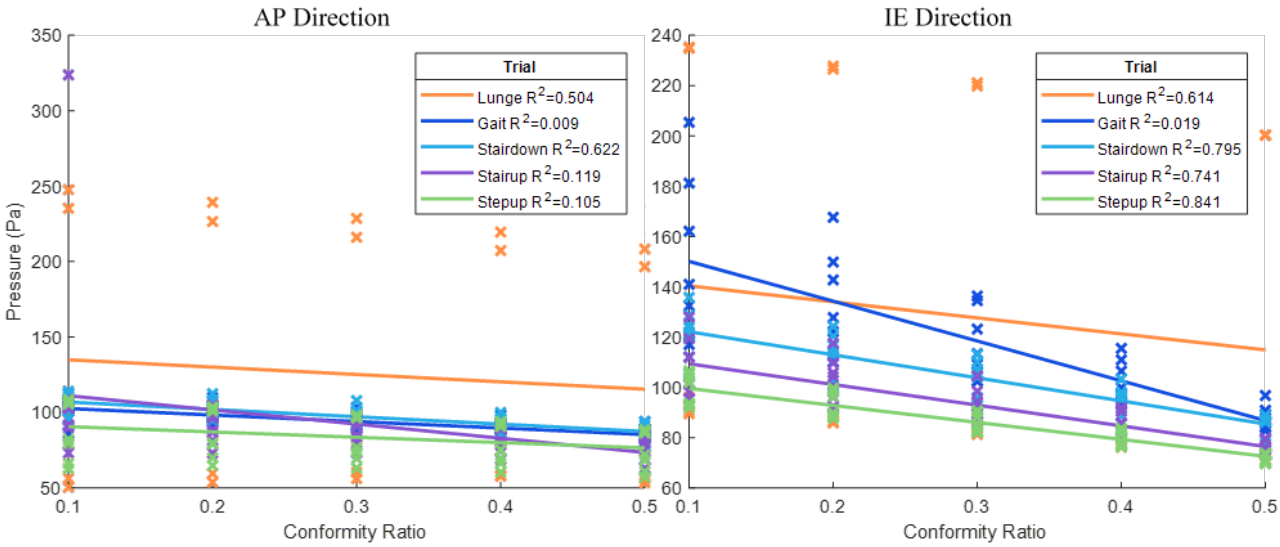

Figure 2-12. Tibiofemoral joint contact pressure regression analysis across all activities, showing AP and IE loading directions

For the ANOVA comparison, differences in tibiofemoral contact pressure were statistically significant when comparing conformities of 0.5 and 0.4 to the least conforming implant (CR = 0.1). The patient implant showed significantly greater contact pressure when compared to all generated implants (Figure 2-13).

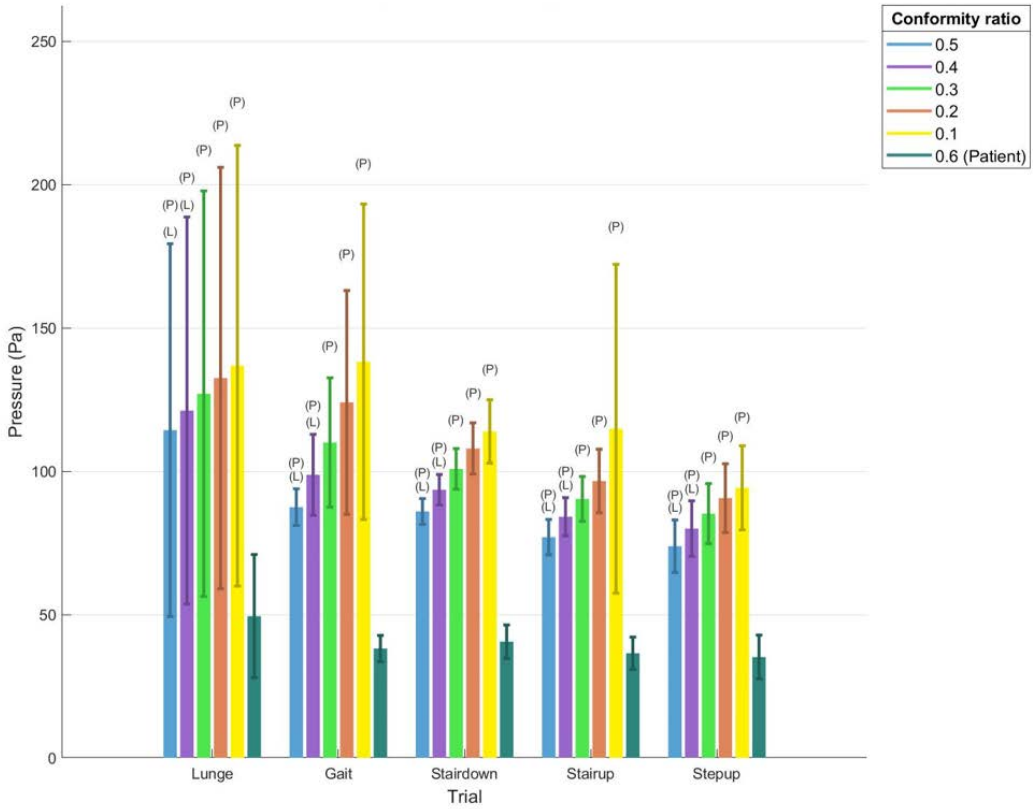

Figure 2-13. Tibiofemoral joint contact pressure for each trial type showing mean and standard deviation. (P), (L) indicates significant difference (P<0.05) from patient implant and least conforming (CR=0.1) implants respectively.

Regression analysis between patellofemoral joint contact pressure and conformity ratio showed patellofemoral contact pressure to increase with decreasing conformity. The strength of this correlation was stronger in IE tests, where R-squared values ranged from 0.26 to 0.55, compared to AP directed tests, where R-squared values were less than 0.1 (Figure 2-14).

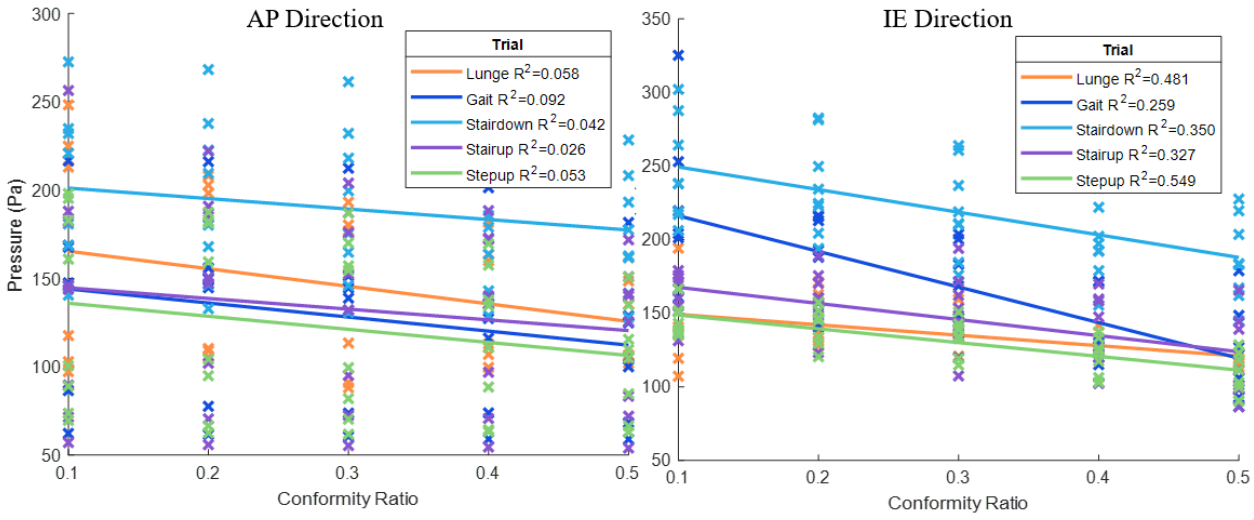

Figure 2-13. Tibiofemoral joint contact pressure regression analysis across all activities, showing AP and IE loading directions

For the ANOVA comparison, the results were as with tibiofemoral contact pressure, with differences in patellofemoral contact pressure statistically significant when comparing conformities of 0.5 and 0.4 to the least conforming implant (CR = 0.1). The patient implant showed significantly greater contact pressure when compared to all generated implants (Figure 2-15).

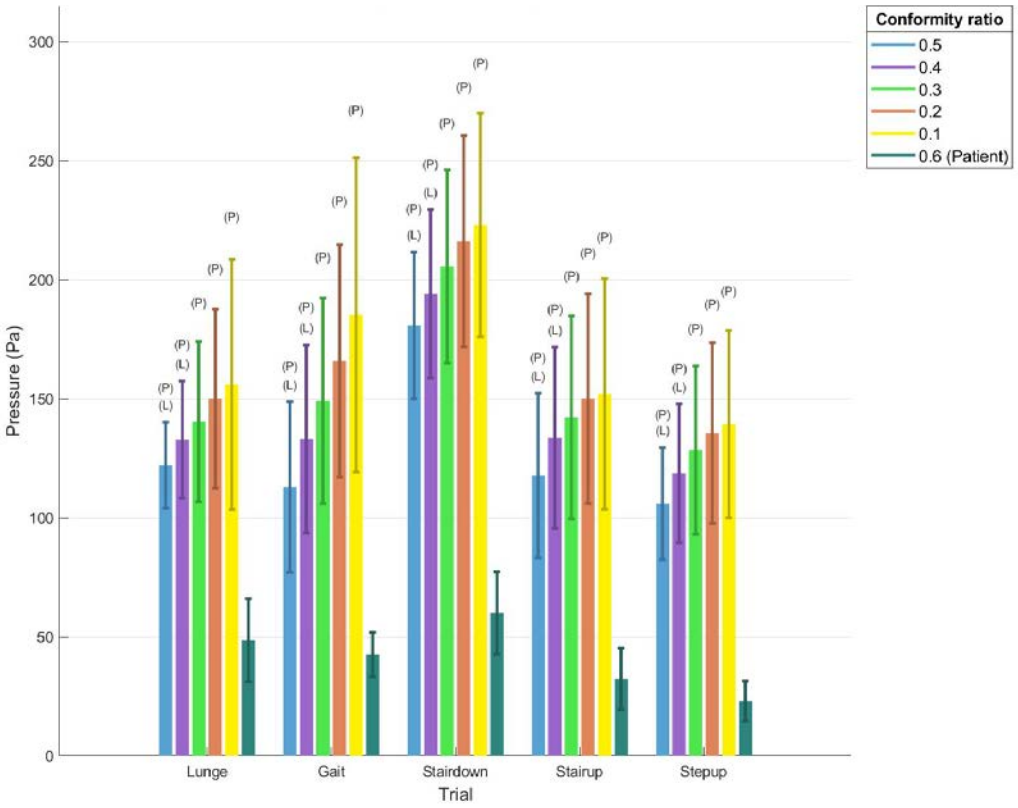

Figure 2-14. Patellofemoral joint contact pressure for each trial type showing mean and standard deviation. (P), (L) indicates significant difference (P<0.05) from patient implant and least conforming (CR=0.1) implants respectively

Total Joint Load

A slight increase in the total joint load was seen in AP directed tested with decreasing conformity, with little trend observed in the IE directed tests. Across all activities and loading directions correlations were weak, with R-squared values less than 0.3 in IE directed tests and 0.1 in AP directed tests (Figure 2-16). The differences observed were not found to be statistically significant (Figure 2-17).

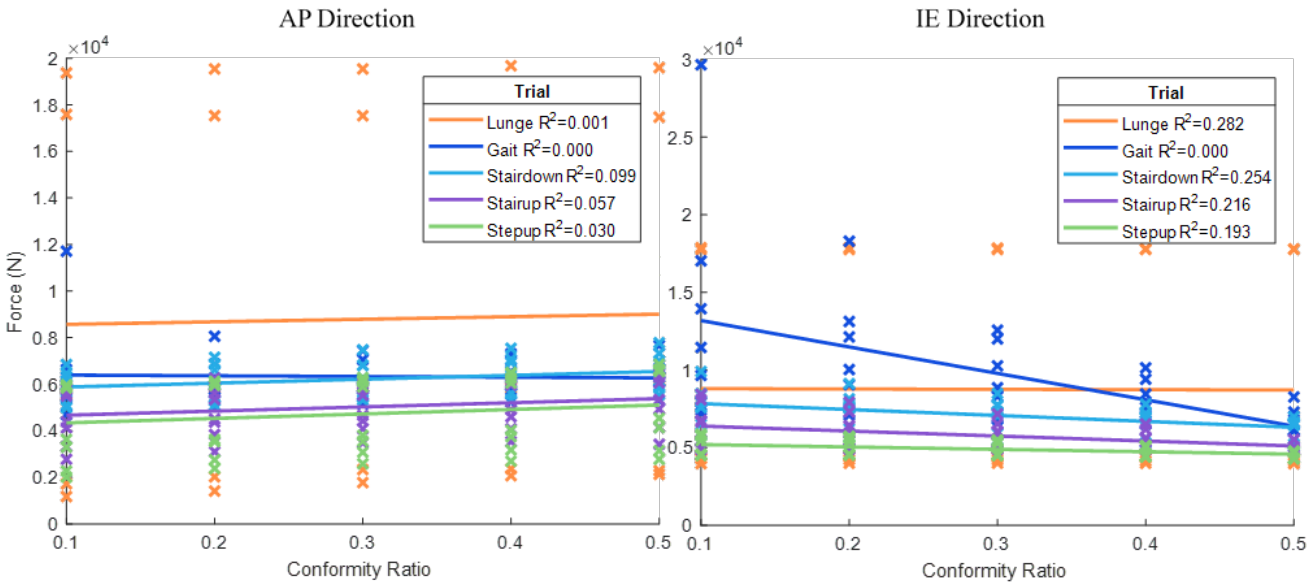

Figure 2-15. Tibiofemoral joint load regression analysis across all activities, showing AP and IE loading directions

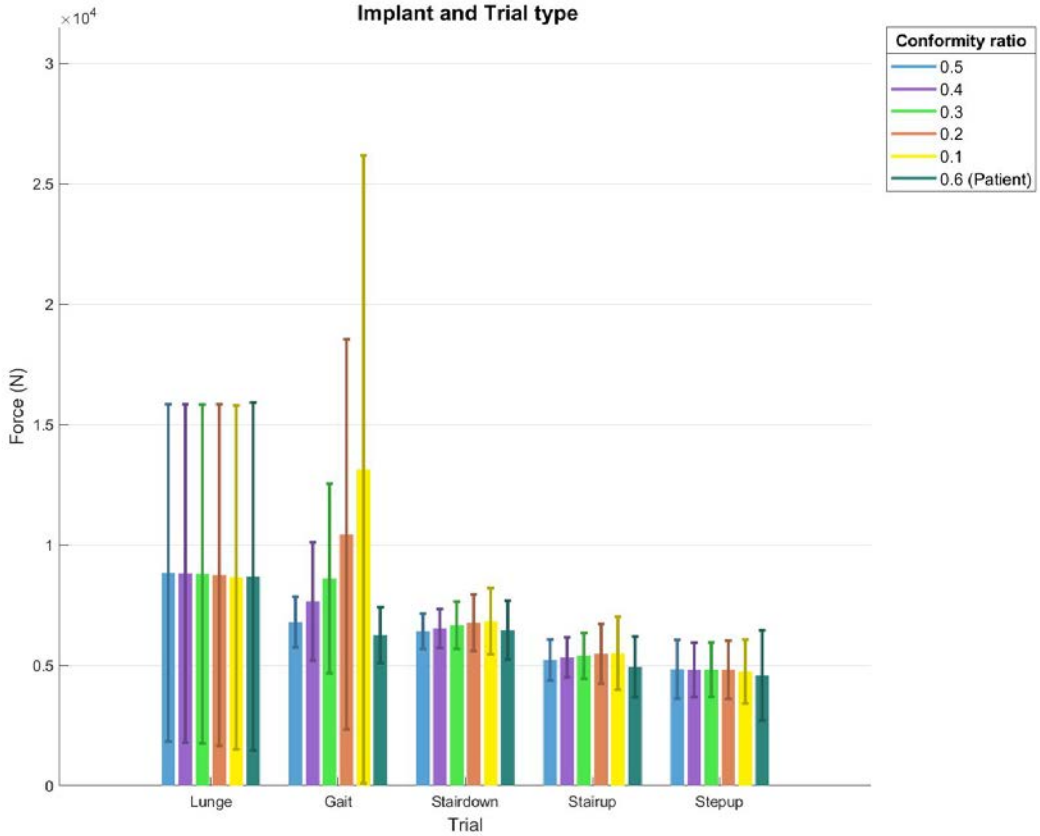

Figure 2-16. Tibiofemoral joint axial load for each trial type showing mean and standard deviation.

2.4 Discussion

This study aimed to objectively quantify the muscle force requirements required to maintain a consistent level of joint stability with changes in implant conformity. In doing so, a physiologically relevant method of evaluating implant laxity is offered that accounts for the muscle force adaptations necessary to prevent excessive joint motion during dynamic activities.

A significant variable impacting stability is implant design and geometry (Blaha, 2004; Soeno et al., 2018). Highly conforming designs promote stability, seen as a reduction in AP or IE displacement translation during laxity testing (Clary et al., 2013; Daniilidis et al., 2012). In this study, a decrease in implant conformity was shown to require significantly greater muscle force to achieve the same displacement profile. Increased muscular demand is problematic in TKR patients, who typically present with loss of muscle strength and function pre and post operatively (Davidson et al., 2013; Thomas et al., 2017; Walsh et al., 1998). Quadriceps strength deficits of 50–60% have been found one month postoperatively (Mizner et al., 2005) and strength deficits continue to persist years after surgery (Silva et al., 2003). For patients presenting with such muscle weaknesses and limitations, there is a likely benefit in the choice of a more conforming implant design to reduce the demand on the musculoskeletal system.

Although the relationship between muscle force and implant conformity has not been examined previously, other studies have shown a reduction in conformity to reduce implant wear, explained by a higher contact area with increasing conformity, (Abdelgaied et al., 2014; Brockett et al., 2017) consistent with the present study. The increased muscle load with decreasing conformity is hypothesized to explain the corresponding increase in

total joint load and via greater compression across the joint. Similarly, the increase in patellofemoral and tibiofemoral contact pressure seen with decreasing conformity is a likely consequence of increased muscle co-contraction (Biscarini et al., 2013; Imran and O'Connor, 1998; Li et al., 1999).

The computationally generated implants were seen to differ significantly from the patient implant design for the joint contact metrics examined. The patient implant saw significantly higher contact areas and lower contact pressures across the tibiofemoral and patellofemoral joints, whilst the total joint load remained comparable to the generated implants. The generated implant was a simplistic design with little account for other geometric paraments to optimize contact mechanics that were likely included in the patient implant. These results highlight the significance of the implant design aside from the level of implant conformity in influencing joint contact metrics. The patient implant (CR = 0.6) was however consistent with the trend for normalized muscle force requirements seen in the generated implants, having lower values than implants with a CR = 0.4 or less across all activities, suggesting that implant conformity is a significant predictor of muscle force requirements over other implant design parameters.

There are some limitations to acknowledge in our model. Firstly, the fluoroscopic data used to validate unconstrained knee joint kinematics was only available for a subset of the activities examined and not all key instances within these activities was provided. However, the RMS errors produced when comparing with available data were reasonable, and it is expected that this trend would be consistent across all activity instances.

Data from a single subject was used in this study, which could limit the applicability of the results, and many model parameters such as ligaments and muscle representations were simplified. In counter to this, maintaining consistency in the model meant the only variable changed was the implant conformity such that changes in observed results can be directly attributed to changes in the CR. Such simplifications also reduced the time and computational cost of this study.

Lastly, this study looked at normalized muscle force for a combined load of selected muscles, with the distribution of load assumed to remain constant through the duration of the laxity test. It is plausible that this distribution would vary during the test and future work could examine muscle contributions individually. Future research is also needed to better determine the level of stability in the healthy natural knee to provide a standard for comparison.

CONCLUSION

3.1 Summary

The research goals of this study were to quantitatively evaluate the muscle force requirements needed to maintain a consistent level of joint stability with changes in implant conformity. In doing so, the gap in current knowledge regarding the relationship between musculoskeletal adaptation patterns and joint stability was addressed. A patient specific, full body finite element model was utilized to perform laxity testing at key loading instances during activities of daily living.

Key findings include:

- A decrease in implant conformity required greater muscle force to achieve the same target kinematic profile. On average as implant conformity increased by 0.1, muscle force requirements were reduced by 10.4%. This trend was consistent across patient and generated implant designs, suggesting that implant conformity is a significant predictor of muscle force requirements over other implant design parameters.
- With decreasing implant conformity, tibiofemoral contact area decreased whilst patellofemoral contact area increased. The decrease in the tibiofemoral contact area is most likely due to reduced contact between components as a consequence of decreasing conformity. The increase in patellofemoral contact area was likely due to increased muscular contraction across the joint which would increase contact area between the femur and patella, with the conformity fixed between

these two components. Both tibiofemoral and patellofemoral contact pressure were seen to increase with decreasing conformity, also a likely consequence of increased muscular contraction across the joint.

- An increase in total joint load was observed with decreasing conformity for most activities and was most significant for the gait activity. Increased joint load is also a likely consequence of greater muscular contraction across the joint with decreasing conformity. It is likely a more significant trend was seen in the gait activity as this activity involved lower flexion angles such that increased muscle contraction would translate more directly to axial load across the joint.
- The computationally generated implants were seen to differ significantly from the patient implant design for the joint contact metrics examined, highlighting the significance of the implant design aside from the level of implant conformity in influencing joint contact metrics.

Increased muscular demand is problematic in TKR patients, who typically present with loss of muscle strength and function pre and post operatively (Davidson et al., 2013; Thomas et al., 2017; Walsh et al., 1998). Quadriceps strength deficits of 50–60% have been found one month postoperatively (Mizner et al., 2005) and strength deficits continue to persist years after surgery (Silva et al., 2003). For patients presenting with such muscle weaknesses and limitations, there is a likely benefit in the choice of a more conforming implant design to reduce the demand on the musculoskeletal system. However, the individual needs of the patient and the conflicting requirements of implant stability and knee range of motion must also be considered. Implant bearing surfaces designed with a high degree of conformity have the potential to be over-constrained (Sathasivam and

Walker, 1999). Lower conforming designs typically allow for greater relative tibiofemoral motion and consequently greater knee flexion, with an additional 1.4 degrees of flexion achieved for each millimeter of posterior femoral translation (Banks et al., 2003a). The conflicting requirements of laxity and conformity in total knee replacements has been investigated with regards to implant wear in prior research, whereby a highly conforming, wear resistant design is seen to reduce stress and wear in the tibial component during gait simulation, however has lower rotational laxity compared to the natural knee (Sathasivam and Walker, 1999). Thus, younger patients who need higher mobility will require less conforming designs to facilitate their wide range of activities, whilst elderly patients with lower physical activity, muscle strength and function will likely benefit from a more constrained design.

The FE model was able to be verified via accurate reproduction of patient knee kinematics when compared to fluoroscopic data, with RMS translational errors less than 1.2mm and rotational errors less than 4.1° for the examined activities of daily living. Other studies have looked at stability in both the natural and implanted knee and seen good agreement between models and experimental data. A combined experimental and computational subject specific analysis was carried out on laxity in the natural knee over five flexion angles from 0-60°, utilizing four cadaveric models for calibration (Harris et al., 2016). Errors between model and experimental kinematics averaged less than 6° during IE rotations, and less than 2.2mm of translation during AP displacements for the intact knees, which is greater than errors between the model and fluoroscopic data seen in this study. In the implanted knee, validation of a six DOF VIVO™ simulator used for implant testing of two implant designs and three dynamic activities was also achieved

with RMS differences in anterior-posterior translations and internal-external rotations less than 1.7mm and 1.4°, respectively (Fitzpatrick et al., 2016).

PI control was an effective method to determine the required muscle loads to achieve a target kinematic profile. Accuracies were within 0.2 mm for AP tests and 0.37° for IE tests when compraing target vs. actual displacements during laxity testing. Forward driven muscle control has been utilized in other studies on knee joint stability. Thelen et al. used a computational model with six DOF joints to estimate dynamic muscle forces in the healthy knee during gait (Thelen et al., 2014). Computed muscle control was used to modulate lower limb muscle excitations such that the simulation closely tracked the measured hip, knee, and ankle angles. The resulting simulations predicted the muscle forces, ligament forces, secondary knee kinematics, and tibiofemoral contact loads. Results were seen to be of comparable magnitude to experimental measures. A similar study utilized computed muscle control to simulate human walking from experimental data and saw RMS kinematics errors in joint kinematics to be generally less than 1° (Thelen and Anderson, 2006). For the implanted knee, a dynamic finite element model of the Kansas knee simulator with PI controlled quadriceps actuation was used to compare experimental and model-predicted whole joint knee mechanics and simulator responses (Baldwin et al., 2012). Errors between model and experimental kinematics averaged 2.4 deg for IE rotation, and 2.4mm for AP translation, which is of comparable magnitude to errors in this study. These studies, along with the current research demonstrate the potential for feedback driven neuromuscular dynamics as a powerful research tool for virtual assessment of biomechanical measures and investigation into influence of physiological, surgical, and design factors on in vivo musculoskeletal loads.

3.2 Limitations

Several limitations and simplifications associated with the current work should be considered. Ligament and muscle properties were not subject specific and were somewhat simplified. All except four of the 44 muscles used in the patient specific FE model were simplified as 1D axial connector elements which are unable to model realistic muscle wrapping. Ligament origin and insertion points were located manually to fit the patients' bone geometries according to anatomic descriptions, and it was not known how the ligament tension was affected by the surgery and whether native soft tissue balance was maintained. Consequently, these approximations might affect the observed results. However, such simplifications were consistent across all laxity tests and thus changes in observed results can be directly attributed to changes in the implant design.

In determining the initial muscle forces for the PI controller via inverse dynamics, the OpenSim calculation does not take into the account the potential loss in muscle strength seen in patients with total knee replacement. An average of 31% strength reduction for isometric knee flexion and extension for patients who undergo TKR has been reported, with up to 40% reduction for full extension (Silva et al., 2003). Knee contact force predictions were shown to improve when knee strength is reduced by 35% to account for weakening as a result of TKR (Marra et al., 2015).

3.3 Future work

Use of data from a single test subject in developing the patient specific model could limit the applicability of these results. A probabilistic FE study highlighted the importance of patient variability, showing subject-specific factors to contribute

substantially to joint loads, quadriceps force and tibiofemoral kinematics (Fitzpatrick et al., 2012). Future work should be done to investigate the influence of patient variability and confirm that the results observed are consistent across a wider population.

In addition, large intra- and inter-subject variations exist for soft tissue properties. Three-dimensional representation of muscle geometries (Blemker and Delp, 2005) and the variability of the subject's soft tissue properties should be considered in future work. Whether the muscle forces required to achieve target kinematics using PI control were physiologically feasible remains to be determined and a more advanced control system that includes such limitations could be included in future. In this study, total muscle force requirements averaged 2750N across all trials. This result is similar with the total muscle force required in a similar study which utilized a set of 13 muscles surrounding the knee joint to dynamically match a target kinematic profile. Up to 3500N was required for some implant designs, however a large variation was seen depending on the implant design and trial type (Rullkoetter et al., 2017). Another variable to be examined is the distribution of the load among the controlled muscles which was set to be fixed in this study. A more advanced model could allow the load distribution to vary and/or examine muscle contributions individually.

To better validate muscle force predictions, it is recommended that the OpenSim static optimization results are compared to EMG muscle force data for the key muscles surrounding the knee joint that were subject to PI control. Ensuring that the timing of muscle activation/deactivation are consistent, and that muscle magnitudes and patterns are good agreement would provide greater confidence in the muscle force predictions.

Although high conformity has been shown to be advantageous in reducing demands on the musculoskeletal system, an optimal balance of stability and joint motion is desired which should be investigated further. Further research should examine the effect of implant conformity on knee joint laxity in conjunction with dynamic muscular loading. In addition, future work is needed to better determine the level of stability in the healthy natural knee to provide stability targets for implants to reproduce optimal patient function.

In this study, the highest implant conformity was a ratio of 0.6 between the femoral component and tibial tray radii. This value was chosen as a baseline model as it was consistent with the conformity ratio of the PFC sigma implant of the test subject in the provided dataset and was of comparable magnitude to implants in the current market which have been found to range from 0.22 to 0.88 (Sintini et al., 2018). However, future work could examine the effect of higher conformities on muscle loading requirements in conjunction with joint range of motion.

REFERENCES

Abaqus 6.14 Online Documentation [WWW Document], 2013. . Dassault Systèmes, 2014. URL http://ivt-abaqusdoc.ivt.ntnu.no:2080/texis/search/?query=wetting&submit.x=0&submit.y=0&group=bk&CDB=v6.14

Abdelgaied, A., Brockett, C.L., Liu, F., Jennings, L.M., Jin, Z., Fisher, J., 2014. The effect of insert conformity and material on total knee replacement wear. Proc. Inst. Mech. Eng. Part H J. Eng. Med. 228, 98–106.

Abulhasan, J., Grey, M., 2017. Anatomy and Physiology of Knee Stability. J. Funct. Morphol. Kinesiol. 2, 1–11.

Ackermann, M., 2007. Dynamics and Energetics of Walking with Prosthesis. Inst. Eng. Comput. Mech. Univ. Stuttgart.

Anderson, F., Guendelman, E., Habib, A., Hammer, S., Holzbaur, K., John, C., Ku, J., Liu, M., Loan, P., Reinbolt, J., Seth, A., Delp S., 2011. How Inverse Kinematics Works [WWW Document]. OpenSim Documentation. URL https://simtk-confluence.stanford.edu:8443/display/OpenSim/How Inverse Kinematics Works

Asano, T., 2004. Knee Simulator Wear Of Cross-Linked UHMWPE In Malrotation Kinematics. Orthop. Proc. 86–B, 438.

Baldwin, M.A., Clary, C.W., Fitzpatrick, C.K., Deacy, J.S., Maletsky, L.P., Rullkoetter, 2012. Dynamic finite element knee simulation for evaluation of knee replacement mechanics. J. Biomech. 45, 474-83.

Banks, S.A., Bellemans, J., Nozaki, H., Whiteside, L.A., Harman, M., Hodge, W.A., 2003a. Knee motions during maximum flexion in fixed and mobile-bearing arthroplasties. Clinical Orthopaedics and Related Research. 410, 131-8.

Banks, S.A., Harman, M.K., Bellemans, J., Hodge, W.A., 2003b. Making sense of knee arthroplasty kinematics: News you can us. Journal of Bone and Joint Surgery, 85-A Suppl 4, 64-72.

Banks, S.A., Hodge, W.A., 2004. Design and activity dependence of kinematics in fixed and mobile-bearing knee arthroplasties. J. Arthroplasty 19, 809–816.

Bartel, D.L., Rawlinson, J.J., Burstein, A.H., Ranawat, C.S., Flynn Jr., W.F., 2005. Designation: F 1223-05 Standard Test Method for Determination of Total Knee Replacement Stresses in polyethylene components of contemporary total knee replacements. Am. Soc. Test. Mater. Int. Jan, 76–82.

Benedetti, M.G., Catani, F., Bilotta, T.W., Marcacci, M., Mariani, E., Giannini, S., 2003. Muscle activation pattern and gait biomechanics after total knee replacement. Clin. Biomech. 18, 871–876.

Biscarini, A., Botti, F.M., Pettorossi, V.E., 2013. Selective contribution of each hamstring muscle to anterior cruciate ligament protection and tibiofemoral joint stability in leg-extension exercise: A simulation study. Eur. J. Appl. Physiol. 2263–2273.

Blaha, J.D., 2004. The rationale for a total knee implant that confers anteroposterior stability throughout range of motion. Journal of Arthroplasty. 19, 22-6.

Blemker, S.S., Delp, S.L., 2005. Three-Dimensional Representation of Complex Muscle Architectures and Geometries. Ann. Biomed. Eng. 33, 661–73.

Bourne, R.B., Chesworth, B.M., Davis, A.M., Mahomed, N.N., Charron, K.D.J., 2010. Patient satisfaction after total knee arthroplasty: Who is satisfied and who is not? Clinical Orthopaedics and Related Research. 468, 57-63.

Brockett, C.L., Carbone, S., Fisher, J., Jennings, L.M., 2017. Influence of conformity on the wear of total knee replacement: An experimental study. Proceedings of the Institution of Mechanical Engineers, Part H: Journal of Engineering in Medicine. 232, 127–134.

Chmielewski, T.L., Rudolph, K.S., Snyder-Mackler, L., 2002. Development of dynamic knee stability after acute ACL injury. J. Electromyogr. Kinesiol. 12, 267–74.

Clary, C.W., Fitzpatrick, C.K., Maletsky, L.P., Rullkoetter, P.J., 2013. The influence of total knee arthroplasty geometry on mid-flexion stability: An experimental and finite element study. J. Biomech. 46, 1351–1357.

Daniilidis, K., Skwara, A., Vieth, V., Fuchs-Winkelmann, S., Heindel, W., Stückmann, V., Tibesku, C.O., 2012. Highly conforming polyethylene inlays reduce the in vivo variability of knee joint kinematics after total knee arthroplasty. Knee 19, 260–265.

Davidson, B.S., Judd, D.L., Thomas, A.C., Mizner, R.L., Eckhoff, D.G., Stevens-Lapsley, J.E., 2013. Muscle activation and coactivation during five-time-sit-to-stand movement in patients undergoing total knee arthroplasty. J. Electromyogr. Kinesiol. 23, 1485–1493.

Dawson, J., Fitzpatrick, R., Murray, D., Carr, A., 1998. Questionnaire on the perceptions of patients about total knee replacement. J. Bone Jt. Surg. 80, 63–9.

Delp, S.L., Anderson, F.C., Arnold, A.S., Loan, P., Habib, A., John, C.T., Guendelman, E., Thelen, D.G., 2007. OpenSim: Open-source software to create and analyze dynamic simulations of movement. IEEE Trans. Biomed. Eng. 54, 1940–1950.

Delp, S.L., Loan, J.P., 1995. A graphics-based software system to develop and analyze models of musculoskeletal structures. Comput. Biol. Med. 25, 21–34.

Delport, H.P., 2006. A kinematic comparison of fixed- and mobile-bearing knee replacements. J. Bone Jt. Surg. (Br). 88, 1016–21.

Dennis, D.A., Komistek, R.D., Mahfouz, M.R., 2003. In vivo fluoroscopic analysis of fixed-bearing total knee replacements. Clin. Orthop. Relat. Res. 410, 114–30.

Desjardins, J.D., Walker, P.S., Haider, H., Perry, J., 2000. The use of a force-controlled dynamic knee simulator to quantify the mechanical performance of total knee replacement designs during functional activity. J. Biomech. 33, 1231–42.

Farquhar, S.J., Reisman, D.S., Snyder-Mackler, L., 2008. Persistence of Altered Movement Patterns During a Sit-to-Stand Task 1 Year Following Unilateral Total Knee Arthroplasty. Phys. Ther. 88, 567–579.

Felson, D.T., Niu, J., McClennan, C., Sack, B., Aliabadi, P., Hunter, D.J., Guermazi, A., Englund, M., 2007. Knee buckling: Prevalence, risk factors, and associated limitations in function. Ann. Intern. Med. 147, 534–540.

Fitzpatrick, C.K., Clary, C.W., Rullkoetter, P.J., 2012. The role of patient, surgical, and implant design variation in total knee replacement performance. J. Biomech. 45, 2092–2102.

Fitzpatrick, C.K., Maag, C., Clary, C.W., Metcalfe, A., Langhorn, J., Rullkoetter, P.J., 2016. Validation of a new computational 6-DOF knee simulator during dynamic activities. J. Biomech. 49, 3177-84.

Fleeton, G., Harmer, A.R., Nairn, L., Crosbie, J., March, L., Crawford, R., Van Der Esch, M., Fransen, M., 2016. Self-Reported Knee Instability before and after Total Knee Replacement Surgery. Arthritis Care Res. 68, 463–471.

Fukubayashi, T., Torzilli, P.A., Sherman, M.F., Warren, R.F., 1982. An in vitro biomechanical evaluation of anterior-posterior motion of the knee. Tibial displacement, rotation, and torque. J. Bone Jt. Surg. (Am) 64, 258–264.

Getting Started with Inverse Kinematics [WWW Document], n.d. . OpenSim Doc. URL https://simtk-confluence.stanford.edu/display/OpenSim/Getting+Started+with+Inverse+Kinematics (accessed 3.10.19).

Ghosh, A., Chatterji, U., 2013. An evidence-based review of enhanced recovery after surgery in total knee replacement surgery. J. Perioper. Pract. 95, 386–9.

Grood, E.S., Suntay, W.J., 1983. A Joint Coordinate System for the Clinical Description of Three-Dimensional Motions: Application to the Knee. J. Biomech. Eng. 105, 136–44.

Guo, E.W., Sayeed, Z., Padela, M.T., Qazi, M., Zekaj, M., Schaefer, P., Darwiche, H.F., 2018. Improving Total Joint Replacement with Continuous Quality Improvement Methods and Tools. Orthop. Clin. North Am. 49, 397–403.

Halloran, J.P., Petrella, A.J., Rullkoetter, P.J., 2005. Explicit finite element modeling of total knee replacement mechanics. J. Biomech. 38, 323–331.

Harris, M.D., Cyr, A.J., Ali, A.A., Fitzpatrick, C.K., Rullkoetter, P.J., Maletsky, L.P., Shelburne, K.B., 2016. A Combined Experimental and Computational Approach to Subject-Specific Analysis of Knee Joint Laxity. J. Biomech. Eng. 138, 081004-081004-8.

Hsieh, H.H., Walker, P.S., 1976. Stabilizing mechanisms of the loaded and unloaded knee joint. J. Bone Jt. Surg. Am) 58, 87–93.

Imran, A., O'Connor, J.J., 1998. Control of knee stability after ACL injury or repair: Interaction between hamstrings contraction and tibial translation. Clin. Biomech. 13, 153–162.

International Organization for Standardization., 2014. ISO 14242-1:2014(en), Implants for surgery — Wear of total hip-joint prostheses, in: 12th Conference on Retroviruses and Opportunistic Infections (CROI).

Kenawey, M., Liodakis, E., Krettek, C., Ostermeier, S., Horn, T., Hankemeier, S., 2011. Effect of the lower limb rotational alignment on tibiofemoral contact pressure. Knee Surgery, Sport. Traumatol. Arthrosc. 12, 1851–9.

Kessler, O., Bull, A.M.J., Amis, A.A., 2009. A method to quantify alteration of knee kinematics caused by changes of TKR positioning. J. Biomech. 42, 665–70.

Klein, R., Serpe, L., Kester, A., Edidin, M., Schmalzried, A., Fishkin, Z., Mahoney, O.M., Schmalzried, T.P., 2003. Rotational constraint of posterior-stabilized total knee prostheses. Clin. Orthop. Relat. Res. 410, 82–89.

Kluess, D., Wieding, J., Souffrant, R., 2010. Finite Element Analysis in Orthopaedic Biomechanics, in: Finite Element Analysis. pp. 151–70.

Knee Replacement Surgery [WWW Document], n.d. . Summit Med. Gr. URL https://www.summitmedicalgroup.com/library/adult_health/aha_total_knee_replacement/ (accessed 3.3.19).

Knight, L.A., Pal, S., Coleman, J.C., Bronson, F., Haider, H., Levine, D.L., Taylor, M., Rullkoetter, P.J., 2007. Comparison of long-term numerical and experimental total knee replacement wear during simulated gait loading. J. Biomech. 40, 1550–1558.

Kurtz, S., Ong, K., Lau, E., Mowat, F., Halpern, M., 2007. Projections of primary and revision hip and knee arthroplasty in the United States from 2005 to 2030. J. Bone Jt. Surg. (Am) 89, 780–5.

Lewek, M.D., Ramsey, D.K., Snyder-Mackler, L., Rudolph, K.S., 2005. Knee stabilization in patients with medial compartment knee osteoarthritis. Arthritis Rheum. 52, 2845–2853.

Li, G., DeFrate, L.E., Zayontz, S., Park, S.E., Gill, T.J., 2004. The effect of tibiofemoral joint kinematics on patellofemoral contact pressures under simulated muscle loads. J. Orthop. Res. 22, 801–806.

Li, G., Rudy, T.W., Sakane, M., Kanamori, A., Ma, C.B., Woo, S.L.-Y., 1999. The importance of quadriceps and hamstring muscle loading on knee kinematics and in-situ forces in the ACL. J. Biomech. 32, 395–400.

Liau, J.J., Cheng, C.K., Huang, C.H., Lo, W.H., 2002. The effect of malalignment on stresses in polyethylene component of total knee prostheses - A finite element analysis. Clin. Biomech. 17, 140–6.

Lingard, E. a, Berven, S., Katz, J.N., 2000. Management and care of patients undergoing total knee arthroplasty: variations across different health care settings. Arthritis Care Res. 13, 129–36.

Lloyd, D., Ph, D., Delp, S., Ph, D., Banks, S., Ph, D., 2013. Fourth Grand Challenge Competition To Predict In Vivo Knee Loads : Description Of Available Experimental Data.

Luger, E., Sathasivam, S., Walker, P.S., 1997. Inherent differences in the laxity and stability between the intact knee and total knee replacements. Knee 4, 7–14.

Mahomed, N.N., Barrett, J., Katz, J.N., Baron, J.A., Wright, J., Losina, E., 2005. Epidemiology of total knee replacement in the United States medicare population. J. Bone Jt. Surg. (Am) 87, 1222–8.

Mahoney, O.M., McClung, C.D., Dela Rosa, M.A., Schmalzried, T.P., 2002. The effect of total knee arthroplasty design on extensor mechanism function. J. Arthroplasty 17, 416–421.

Maletsky, L.P., Hillberry, B.M., 2005. Simulating Dynamic Activities Using a Five-Axis Knee Simulator. J. Biomech. Eng. 127, 123–33.

Markolf, K.L., Bargar, W.L., Shoemaker, S.C., Amstutz, H.C., 1981. The role of joint load in knee stability. J. Bone Jt. Surg. (Am) 63, 570–585.

Markolf, K.L., Graff-Radford, A., Amstutz, H.C., 1978. In vivo knee stability. A quantitative assessment using an instrumented clinical testing apparatus. J. Bone Jt. Surg. (Am) 60, 664–674.

Marra, M.A., Vanheule, V., Fluit, R., Koopman, B.H.F.J.M., Rasmussen, J., Verdonschot, N., Andersen, M.S., 2015. A subject-specific musculoskeletal modeling framework to predict in vivo mechanics of total knee arthroplasty. J. Biomech. Eng. 137, 020904-020904-12.

Mizner, R.L., Petterson, S.C., Stevens, J.E., Vandenborne, K., Snyder-Mackler, L., 2005. Early quadriceps strength loss after total knee arthroplasty: The contributions of muscle atrophy and failure of voluntary muscle activation. J. Bone Jt. Surg. (Am) 87, 1047–1053.

Moran, M.F., Bhimji, S., Racanelli, J., Piazza, S.J., 2008. Computational assessment of constraint in total knee replacement. J. Biomech. 41, 2013–2020.

Multiple comparison test [WWW Document], n.d. . MATLAB Doc. URL https://www.mathworks.com/help/stats/multcompare.html (accessed 3.23.19).

Musculature [WWW Document], n.d. . Kinesiology. URL http://aptsaweb.org/hmchai/Kinesiology/KINmotion/Musculature.htm (accessed 3.3.19).

Nam, D., Nunley, R.M., Barrack, R.L., 2014. Patient dissatisfaction following total knee replacement. A growing concern? Bone Joint J. 96, 96–100.

Noble, P.C., Gordon, M.J., Weiss, J.M., Reddix, R.N., Conditt, M.A., Mathis, K.B., 2005. Does total knee replacement restore normal knee function? Clin. Orthop. Relat. Res. 431, 157–65.

Petterson, S.C., Mizner, R.L., Stevens, J.E., Raisis, L.E.O., Bodenstab, A., Newcomb, W., Snyder-Mackler, L., 2009. Improved function from progressive strengthening interventions after total knee arthroplasty: A randomized clinical trial with an imbedded prospective cohort. Arthritis Care Res. 61, 174–183.

Reinders, J., Sonntag, R., Kretzer, J.P., 2014. Wear behavior of an unstable knee: stabilization via implant design? J. Biomed. Biotechnol. 821475.

Rullkoetter, P.J., Fitzpatrick, C.K., Clary, C.W., 2017. How can we use computational modeling to improve total knee arthroplasty? Modeling stability and mobility in the implanted knee. J. Am. Acad. Orthop. Surg. 25, S33–S39.

Sathasivam, S., Walker, P.S., 1999. The conflicting requirements of laxity and conformity in total knee replacement. J. Biomech. 32, 239–247.

Schmitt, L.C., Fitzgerald, G.K., Reisman, A.S., Rudolph, K.S., 2008. Instability, Laxity, and Physical Function in Patients With Medial Knee Osteoarthritis. Phys. Ther. 88, 1506–1516.

Schmitt, L.C., Rudolph, K.S., 2008. Muscle stabilization strategies in people with medial knee osteoarthritis: the effect of instability. J. Orthop. Res. 26, 1180–1185.

Schutte, L.M., Rodgers, M.M., Zajac, F.E., Glaser, R.M., 1993. Improving the efficacy of electrical stimulation-induced leg cycle ergometry: An analysis based on a dynamic musculoskeletal model. IEEE Trans. Rehabil. Eng. 1, 109–25.

Schwab, J.H., Haidukewych, G.J., Hanssen, A.D., Jacofsky, D.J., Pagnano, M.W., 2005. Flexion instability without dislocation after posterior stabilized total knees. Clin. Orthop. Relat. Res. 440, 96–100.

Severijns, P., Vanslembrouck, M., Vermulst, J., Callewaert, B., Innocenti, B., Desloovere, K., Vandenneucker, H., Scheys, L., 2016. High-demand motor tasks are more sensitive to detect persisting alterations in muscle activation following total knee replacement. Gait Posture 50, 151–158.

Shu, L., Yamamoto, K., Yao, J., Saraswat, P., Liu, Y., Mitsuishi, M., Sugita, N., 2018. A subject-specific finite element musculoskeletal framework for mechanics analysis of a total knee replacement. J. Biomech. 77, 146–154.

Silva, M., Shepherd, E.F., Jackson, W.O., Pratt, J.A., McClung, C.D., Schmalzried, T.P., 2003. Knee strength after total knee arthroplasty. J. Arthroplasty 18, 605–11.

Sintini, I., Fitzpatrick, C.K., Clary, C.W., Castelli, V.P., Rullkoetter, P.J., 2018. Computational evaluation of TKR stability using feedback-controlled compressive loading. J. Orthop. Res. 36, 1901-9.

Soeno, T., Mochizuki, T., Tanifuji, O., Koga, H., Murayama, T., Hijikata, H., Takahashi, Y., Endo, N., 2018. No differences in objective dynamic instability during acceleration of the knee with or without subjective instability post-Total knee arthroplasty. PLoS One 13, 1–12.

Stiehl, J.B., Haas, B.D., Mahfouz, M.R., Komistek, R.D., Dennis, D.A., 2003. Conventry Award Paper: Multicenter Determination of In Vivo Kinematics After Total Knee Arthroplasty. Clin. Orthop. Relat. Res. 416, 37–57.

Thelen, D.G., Anderson, F.C., 2006. Using computed muscle control to generate forward dynamic simulations of human walking from experimental data. J. Biomech. 39, 1107–1115.

Thelen, D.G., Won Choi, K., Schmitz, A.M., 2014. Co-Simulation of Neuromuscular Dynamics and Knee Mechanics During Human Walking. J. Biomech. Eng. 136, 021033.

Thomas, A.C., Judda, D.L., Davidsonb, B.S., Eckhoffc, D.G., Stevens-Lapsley, J.E., 2017. Quadriceps/hamstrings co-activation increases early after total knee arthroplasty. Knee 21, 1115–1119.

Verstraete, M.A., Victor, J., 2015. Possibilities and limitations of novel in-vitro knee simulator. J. Biomech. 48, 3377–3382.

Walker, P.S., Haider, H., 2003. Characterizing the motion of total knee replacements in laboratory tests. Clinical Orthopaedics and Related Research. 410, 54–68.

Walker, P.S., Zhou, X.M., 1987. Inherent laxity in total knee prostheses. J. Arthroplasty 2, 199–207.

Walsh, M., Woodhouse, L.J., Thomas, S.G., Finch, E., 1998. Physical impairments and functional limitations: A comparison of individuals 1 year after total knee arthroplasty with control subjects. Phys. Ther. 78, 248–258.

Wang, C.-J., Walker, P.S., 1974. Rotatory laxity of the human knee joint. J. Bone Joint Surgery (Am) 56, 161–70.

Waslewski, G.L., Marson, B.M., Benjamin, J.B., 1998. Early, incapacitating instability of posterior cruciate ligament-retaining total knee arthroplasty. J. Arthroplasty 13, 763–767.